NASA Technical Paper 2966

March
1990

Simulated-Airline-Service Flight Tests of Laminar-Flow Control With Perforated-Surface Suction System

Dal V. Maddalon
Langley Research Center
Hampton, Virginia

Albert L. Braslow
Analytical Systems & Materials, Inc.
Hampton, Virginia

National Aeronautics and
Space Administration
Office of Management
Scientific and Technical
Information Division

Summary

The effectiveness and practicality of leading-edge systems for suction laminar-flow control on transport airplanes have been investigated in a NASA flight-test program utilizing a modified JetStar airplane. The leading-edge region imposes the most severe conditions on systems required for any type of laminar-flow control. Tests of the leading-edge systems, therefore, provided definitive results as to the feasibility of active laminar-flow control on airplanes. The test airplane was operated under commercial transport operating procedures from various commercial airports and at various seasons of the year.

Two types of suction system with their related subsystems were investigated—suction through multiple slots and suction through surface perforations. Results with the perforated-surface suction system are reported herein. The flight tests demonstrated successful packaging of required systems into the wing leading-edge volume anticipated for small future laminar-flow transports. The flight tests also demonstrated required effectiveness and probable practicality of a perforated-surface suction system in combination with a leading-edge flap and freezing-point depressant for insect contamination avoidance and anti-icing. These results are considered to be a major step forward in the evolution of suction laminar-flow control for transport airplanes.

Introduction

As part of a NASA-industry development program on active laminar-flow control (LFC) with suction, initiated in the mid-1970's, a flight-test program with a modified JetStar airplane was conducted to provide definitive information on the effectiveness and reliability of various LFC subsystems. The leading-edge region of a laminar-flow wing for a high-subsonic-speed transport airplane was selected as the test region because the especially difficult technical and design challenges associated with this region must be overcome before active laminar-flow control can be considered a viable transport design option. In addition, the required subsystems for this region are equally applicable to the concept of hybrid LFC (a combination of active LFC from the leading edge to near the front spar and passive LFC from that point back) and to the concept of active LFC to the more rearward positions. Subsystems that must be integrated into the limited volume of the leading-edge box include those required for boundary-layer suction, avoidance of surface contamination, anti-icing, and purging of fluids from the suction elements. The external wing surfaces must also be exceptionally smooth and capable of resisting the effects of erosion, corrosion, and foreign-object damage. No attempt was made in these tests to maintain laminar flow to positions aft of the wing front spar.

Design, fabrication, and ground testing of various approaches to the required LFC subsystems have been under way for several years in an attempt to develop economical solutions that satisfy the laminar-flow constraints. Developments included both the multiple-slot-surface and the perforated-surface approach to boundary-layer suction. Subsystems with the potential to meet the LFC requirements for both the slotted-surface and the perforated-surface approach were installed in the JetStar leading-edge box regions (slotted on the left wing and perforated on the right wing). The flight-test program included initial checkout of all systems and instrumentation and determination of settings for the suction-air and fluid-flow rates and distributions. The principal effort was demonstration of the ability to attain the design extent of laminar flow under routine operational conditions representative of LFC subsonic commercial transport airplanes and to provide some determination of maintenance requirements.

During simulation of typical transport operations, the suction system was operated in a hands-off mode (except for on-off inputs), and a goal of at least two operations per day was imposed. The airplane was operated in different geographical areas, seasons of the year, and weather conditions in order to impose a variety of representative atmospheric environments. The airplane remained outdoors at all times and no protective measures were taken to lessen the impact of adverse weather or contamination on the test articles. Each flight consisted of ground queuing, taxi, takeoff, climb to cruise altitude, cruise for sufficient time to determine possible atmospheric effects on laminar flow, descent, landing, and taxi, with all conditions representative of airline operations.

Only the system performance aspects for the perforated-surface approach during the simulated airline flights are evaluated herein. Results for the slotted-surface approach and for other associated investigations with the JetStar are included in other reports (e.g., ref. 1). Overviews of the entire program and brief summaries of pertinent flight results for both the slotted-surface and the perforated-surface approach are presented in references 2 to 6.

This Leading-Edge Flight-Test (LEFT) Program was initiated as part of a joint NASA-industry effort on the development of laminar-flow control technology under the NASA Langley Research Center Aircraft Energy Efficiency (ACEE) Program. The authors gratefully acknowledge the significant contributions made during the course of the program

by R. D. Wagner, M. C. Fischer, A. S. Wright, R. S. Baron, and D. F. Fisher of NASA and W. E. Pearce, D. E. McNay, and J. A. Thelander of the Douglas Aircraft Company, McDonnell Douglas Corporation.

Nomenclature

C_L	lift coefficient
C_p	surface pressure coefficient (CP in data snapshot (fig. 10))
C_Q	surface suction coefficient (CQ in data snapshot (fig. 10))
c	chord (C in data snapshot (fig. 10))
g	gravitational acceleration, 32.174 ft/sec^2
H	altitude
LEFT	leading-edge flight test
LETA	leading-edge test article
LFC	laminar-flow control
M	free-stream Mach number
p	pressure
PGME	propylene glycol methyl ether
q	free-stream dynamic pressure
R	free-stream unit Reynolds number
R_θ	attachment-line momentum-thickness Reynolds number
s	streamwise surface distance (S in data snapshot (fig. 10))
SAS	simulated airline service
T	outside ground-level air temperature
t	time
V	free-stream velocity
W.S.	wing spanwise station
x	streamwise chordwise distance (X in data snapshot (fig. 10))
α	angle of attack
η	semispan location, fraction of semispan

Subscript:

tr	transition

Test Article

Systems

The perforated-surface leading-edge test article (LETA), developed and fabricated by the Douglas Aircraft Co., was installed on the right wing of the NASA JetStar airplane and was designed to produce laminar flow on the upper wing surface only to the front spar (13 percent chord) during high-altitude cruise flight. References 6 to 9 describe the perforated-surface LETA developments. Figure 1 presents an exploded view of the principal components. The LETA was faired into the basic JetStar wing surface in the inboard, outboard, and rearward directions with fiberglass fairings. The planform in figure 2 shows that the test article was installed between wing stations 134.750 and 196.000, the original location of the wing fuel tanks. The test article was dimensionally about equivalent to the leading-edge box of a DC-9-30 airplane at the mean aerodynamic chord, an indication that the required systems can be packaged into the volume available in a small commercial transport. Thus one objective of the JetStar program is satisfied. Two photographs of the JetStar airplane showing the perforated-surface LETA are presented in figures 3 and 4.

Suction. The leading-edge surface consisted of suction strips with about 62 percent of the perforated surface open and about 38 percent of the perforated surface blocked where the titanium skin was bonded to the corrugated carbon-fiberglass substructure (fig. 5). An electron-beam process was used to perforate the 0.025-in.-thick titanium skin with a uniform array of 0.0025-in.-diameter holes spaced 0.035 in. apart, yielding a high-quality aerodynamic suction surface. Suction ducts or flutes collected the sucked air, which was then routed to the suction source (refs. 7 and 8). Suction flow from each of 15 flutes (fig. 6) was controlled individually (ref. 10).

Contamination avoidance. The concept selected for avoiding insect contamination consisted of a retractable leading-edge shield (fig. 5) extended during takeoff and landing (at altitudes below approximately 4000 ft). On a transport airplane, this shield may also be designed to act as a Krueger-type high-lift device, although for this experiment it was designed to carry only a small amount of lift because the shield was installed on only one wing. Fluid-spray nozzles were also incorporated on the shield underside to augment the insect-protection effectiveness of the shield; previous analyses and wind-tunnel tests (ref. 7) had indicated that this precaution might be necessary. A fluid solution consisting of 60 percent propylene glycol methyl ether (PGME) and

40 percent water was sprayed from these nozzles onto the wing leading edge at altitudes below approximately 1000 ft at a rate of about 0.2 gal/min for each 1 ft of span (ref. 6). This PGME solution had no measurable effect on the airplane materials used and, because it was a freezing-point depressant, it also provided wing anti-icing.

Anti-icing. As previously indicated, the retractable leading-edge shield and spray nozzles provided the wing with an anti-icing capability when needed. The shield itself was protected from surface icing by a porous surface insert along the shield leading edge. This insert, available commercially, extended around the leading edge a sufficient chordwise distance to include the extremes of the shield attachment-line movement. A freezing-point depressant (ethylene glycol) was ejected through the porous surface when needed during icing conditions. Although different liquids were used for the wing and shield in this flight test, it is expected that the same liquid would be used for both purposes in future applications.

Purging. Because of fluid ejection onto the wing for protection against insect contamination and surface icing, it was necessary to provide a system to remove possible residual fluid from the surface perforations or suction ducting before the suction system was activated at cruise altitudes. The purging system utilized a reversed flow of filtered pressurized air through the suction-system ducting.

Instrumentation

Static and total pressures on or in the test article were measured with electronic scanivalves. Velocity fluctuations inside the boundary layer at various chordwise positions were obtained with surface-mounted hot-film sensors. Mass flow through each suction flute was determined with individually calibrated sonic nozzles described in reference 10. Measurements from the suction pump and other leading-edge systems as well as the basic airplane parameters were obtained with conventional instrumentation. The sizes and quantities of atmospheric particles (e.g., ice and water droplets) encountered in flight were measured with a commercially available laser particle spectrometer (Knollenberg probe), and the mere presence of ice particles was determined with a "charging patch."

Surface static pressure. Surface static pressures were measured at three spanwise positions (fig. 6). Note that the center measurements were made between each suction flute, whereas inboard and outboard measurements were made only between alternate flutes. In general, an unobtrusive sensor installation was made by locating subsurface tubes against the underside of the perforated titanium in the nonporous region between active suction flutes (fig. 6). In a few instances, however, the bonding adhesive blocked the perforated surface, and thus it was necessary to drill conventional orifices 0.0135 in. in diameter. The drilled orifices are identified in the listing of the surface pressure-sensor locations in table 1.

Flute static pressure. Static pressures inside the suction flutes were measured near the midspan of each flute. In addition, internal flute pressures were measured near the inboard and outboard ends of flutes 3, 5, and 11 to indicate spanwise pressure gradients along the flutes. The typical measured spanwise gradient of pressure coefficient was approximately 0.033 per foot; the pressure was more negative inboard.

Boundary-layer total pressure. Twenty total-pressure probes were mounted along the wing span near the LETA trailing edge to determine the approximate chordwise location of transition from laminar to turbulent flow. The probes and tubing were attached to the sensor panel (figs. 1 and 6) and were spaced 3 in. apart in the spanwise direction. The nominal probe height above the surface was 0.060 in., with two additional probes mounted 0.020 and 0.150 in. above the surface at five spanwise stations. A reference total pressure was obtained by averaging the readings of two probes mounted well outside the boundary layer at 2.5 in. above the surface (figs. 4 and 7). The deficit between the pressures from the 0.060-in.-high probe and the average reference pressure was used as an indication of the chordwise position of boundary-layer transition; the pressure differentials were calibrated against transition position artificially fixed by placing three-dimensional roughness elements at various chordwise positions. (See appendix A of ref. 3 for details.) The pressure differential was nearly zero for a laminar boundary layer because the 0.060-in.-high probes were outside the thin laminar layer. A maximum pressure differential was obtained for transition near the wing leading edge. Figure 7 is a photograph of the total-pressure probes, and figure 8 presents predicted ratios of total-pressure differential to free-stream dynamic pressure as a function of transition location for a representative flight condition ($M = 0.75$ and $H = 36\,000$ ft).

Boundary-layer velocity fluctuations. Surface-mounted hot-film sensors were located as shown in figure 6 to measure boundary-layer velocity fluctuations. These data are not analyzed in this paper, but the existence of the sensors is important to

interpretation of some of the data presented because the sensors sometimes affected the local position of boundary-layer transition.

Atmospheric ice crystals. A laser particle spectrometer (Knollenberg probe) was mounted atop a ventral pylon on the fuselage upper surface (fig. 9) to measure ice particles encountered in flight. Particle flux was measured in 30 size categories from 20 to 600 μm in diameter. A description of the probe operation, measuring and testing techniques, and data analysis methods is given in references 2 and 3.

A simple charging-patch device for detection of atmospheric ice particles and the impending loss of laminar flow (ref. 3) was also investigated as a possible low-cost application to future laminar-flow airplanes. The device, mounted on the pylon leading edge (fig. 9), responded to the electrostatic charge developed when ice or water droplets struck the aircraft surface. A device operating on the same principle was previously used on the X-21 research airplanes and detected the presence of clouds when laminar-flow losses occurred.

Results

To expedite analysis of the flight tests, "data snapshots" of continuously recorded (two points per second) data were taken at various time intervals. The data snapshots were typically recorded at 2-minute intervals; however, when transient boundary-layer conditions were under investigation, the time interval between data snapshots was reduced to a few seconds. Further reduction in snapshot time interval or analysis of the continuous data tape was generally unnecessary.

A representative data snapshot is presented in figure 10. The swept-wing planforms in the upper part of the figure schematically represent the LETA and indicate the regions of laminar (clear area) and turbulent (dark area) flow. The plots in the central part of the figure illustrate the chordwise distributions of suction-flow coefficient and the inserted numerical values are the average suction-flow coefficients after multiplication by 10^{-4}. The plots in the lower part of the figure illustrate the chordwise variations of surface pressure coefficient at the center spanwise station for the various cases. The keys with the LETA planform sketches at the top of figure 10 present, from top to bottom, the flight test number, the time of the snapshot during the flight, and the corresponding Mach number, altitude (in feet), Reynolds number per foot, and charging-patch current reading (in microamperes). A current reading inside the range of 0.025 to -0.05 μA correlated with visibly clear flight conditions and zero particle count. The chordwise distributions of suction-flow coefficient that were used were determined for an LFC application with suction aft of mid chord. The control valves were set and were not changed in accordance with the hands-off mode of operation. Plots of chordwise suction distribution and pressure distribution are not repeated in subsequent figures on the extent of laminar flow attained.

Leading-Edge Notch and Bump

Prior to the simulated-airline-service (SAS) flight tests, system checkout tests indicated progressively increased spanwise turbulent-flow contamination along the wing leading edge with increased unit Reynolds number (planforms 2 to 5 in fig. 11). The turbulence contamination emanated from the turbulent fuselage boundary layer. Devices similar to those that have previously been successful in elimination of spanwise turbulence contamination along the attachment line (e.g., ref. 11) were tested. (See fig. 12.) A leading-edge notch-bump configuration at the inboard end of the test article (fig. 13) permitted attainment of laminar flow over the complete test article at Reynolds numbers as large as 2.7×10^6 per foot, which corresponds to altitudes as low as 20 000 ft (planform 1 of fig. 11). All SAS tests were made with this notch-bump configuration. Additional information on spanwise turbulent-flow contamination is presented in the section entitled *Off-Design Conditions.*

Simulated-Airline-Service Flights

Simulated airline service involved a series of flights to and from several commercial airports in the continental United States during various seasons. Home bases were Atlanta, Georgia, for summer testing, Pittsburgh, Pennsylvania, for late summer testing, and Cleveland, Ohio, for winter testing. City pairs 300 to 500 n.mi. apart were selected to provide sufficient cruise time for successful demonstration of sustained laminar flow. Seventy flights to thirty-five airports, indicated in figure 14, were accomplished. Following each landing, the LETA was inspected for insect debris or other contaminants, foreign-object damage, and surface erosion or corrosion. The locations and heights of any insect residue, measured with a right-angle prism microscope, were generally documented as were any instances of LETA cleaning or maintenance. Flight conditions, ice-crystal encounters, extent of laminar flow, system information of special significance, and any data anomalies are summarized for each of these flights in table 2; the flight dates and surface weather conditions at the origin and destination are presented in table 3. Additional detail on cloud conditions encountered during each flight is documented in reference 3.

Discussion

Overall Performance

The SAS flights were, in general, divided into three phases: (1) summer flights in the vicinity of Atlanta, Georgia; (2) late summer flights in the vicinity of Pittsburgh, Pennsylvania; and (3) winter flights in the vicinity of Cleveland, Ohio. The home base for the complete program was the NASA Dryden Flight Research Center at Edwards, California. Cruise flight was nominally at a Mach number of 0.75 and altitudes of 33 000 and 35 000 ft.

The program goal of at least two operations per day was generally accomplished. The breaks in flight testing indicated in table 3 between phases 1 and 2, during phase 2, and during phase 3 were caused by airplane maintenance requirements and not by the LFC systems. In fact, no schedule delays were ever caused by malfunctions of any LFC system, all of which continually performed as intended. No changes were made in suction-valve settings, and the only system inputs were suction on or off, leading-edge flap extended or retracted, insect-protection or anti-icing spray system on or off, and liquid-purge system on or off.

A review of table 2 indicates that the design goal of laminar flow to the front spar was attained at cruise conditions for the vast majority of the flights. Occasional localized or more extensive losses of laminar flow indicated in table 2 are discussed in the following sections, organized in accordance with various factors that affect the attainability and economics of laminar flow.

Surface Disturbances

Fabrication quality. At no time during the SAS flight tests (in fact, at no time during the entire 4-year Leading-Edge Flight-Test (LEFT) Program) did any external imperfections on the LETA caused by fabrication or deterioration of the perforated titanium sheet ever introduce disturbances into the laminar boundary layer that caused transition ahead of the front spar at cruise conditions. Surface discontinuities at some of the surface hot-film sensors, however, were the likely causes of a few occasional localized forward movements of transition.

Indications of this local instrumentation-installation effect were noted at cruise during flights 1091 and 1133 (fig. 15) when transition moved forward of the front spar at spanwise station 4 (station numbers shown in fig. 6) when cruise altitude was reduced to below 27 000 ft. The resulting increase in Reynolds number to greater than 2×10^6 per foot likely increased the roughness Reynolds number to a value larger than critical, that is, the value that caused premature transition. Further reductions in altitude to about 10 000 ft, with further increases in unit Reynolds number (fig. 16), resulted in a forward transition movement at other spanwise stations adjacent to station 4 (stations 1, 2, 3, and 5). This forward movement was most likely due to exceedence of the critical roughness value for other hot-film sensors in this region at the larger unit Reynolds numbers. Transition at the most inboard station may also have been affected by wing-fairing discontinuities at the larger Reynolds numbers. These results show the well-known increased sensitivity of laminar flow to surface irregularities as unit Reynolds number increases. The basic perforated titanium surface, however, was manufactured smooth enough to permit full laminar flow at these large values of unit Reynolds number.

Insect contamination. The effectiveness of the leading-edge shield with the fluid spray system in the prevention of surface insect contamination is clearly shown in figure 17. The measured insect accumulation on the shielded leading edge is compared with that on the slotted configuration with an inoperative anticontamination system during landing. Only two insects impacted the shielded leading edge, and those were in an unprotected region near the inboard end of the shield. These results not only demonstrate shield effectiveness but also indicate the necessity of an anticontamination system during low-altitude flight when insects are present. Figure 18 presents an example of a localized forward transition movement for flight 1069 probably caused by an insect impact during flight 1068, when the anticontamination system was not used because of difficulties unrelated to the LFC system.

Very rarely, an insect of sufficient size to move transition forward impacted the wing when the anticontamination system was in use (e.g., flight 1090, shown in fig. 19). Table 2(b) indicates the presence of a 0.015-in.-high insect inboard near the leading edge after flight 1090; this contamination probably caused the inboard forward transition movement shown in figure 19. After flight 1091, surface inspection revealed a smaller insect at or near the same location as for the previous flight (table 2(b)), an indication of a possible partial erosion of the same insect. Attainment of complete laminar flow inboard during flight 1091 (fig. 15) indicated that the erosion had decreased the height to a value less than critical. The localized forward transition at midspan during flight 1090 (fig. 19) and its elimination during flight 1091 (fig. 15) also indicated the possibility of

erosion of a midspan insect, although the presence of an insect at midspan was not noted during inspection after flight 1090. While the erosion possibility may be a helpful effect, it of course cannot be relied upon in place of an anticontamination device.

The turbulent flow that existed during flight 1079 (table 2(b)) near spanwise station 10 also probably resulted from insect contamination, although presence of insect remains was not documented after this flight. In accordance with experimental rules, the LETA was not cleaned prior to the next takeoff (flight 1080), and figure 10 indicates the continued presence of the disturbance at station 10 through time 10:28:02. After emergence from the ice crystals encountered at time 10:30:02, however, planform 4 of figure 10 indicates reattainment of fully laminar flow at station 10. It appears probable that the surface disturbance that likely existed near station 10 was removed by the abrasive action of the ice crystals.

Flight 1087 (fig. 20) provides further evidence of a possible favorable effect of ice-crystal encounter on surface disturbances. Figure 20 indicates that a probable insect impact during takeoff caused premature transition in the region of the most inboard probe station (t = 9:38:17 and 9:40:30). At the next data time (t = 9:43:05), the charging patch and the partial loss of laminar flow across the span indicated flight through ice crystals. At the next data time (t = 9:45:14), the aircraft had emerged from the ice crystals and full laminar flow was reattained. It appears, then, that an ice-crystal environment, even for short duration, may be sufficient to remove or at least reduce the insect excrescence to a subcritical height.

The importance of preventing insect accumulation in the leading-edge region was clearly shown by a checkout flight preceding the SAS flights. Although it had been shown that the leading-edge notch and bump protected the wing from spanwise turbulence contamination from the fuselage turbulent boundary layer (fig. 11), any accumulation of critical roughness near the attachment line outboard of the device might have caused a spanwise contamination outward from the position of the roughness. Such an occurrence was observed during flight 1045 when the leading-edge shield was retracted prematurely. Figure 21 indicates that inboard accumulation of insect remains caused transition near the leading edge that spread spanwise along the attachment line and caused turbulent flow over almost the entire outboard region. This is indicated in figure 22, which shows that the attachment-line momentum-thickness Reynolds number R_θ exceeded a value of 100 over a large portion of the span at the flight unit Reynolds number of 1.95×10^6. Previous investigations (e.g., ref. 12) have clearly indicated that turbulence will propagate along the attachment line when R_θ exceeds a value of about 95. A decrease in unit Reynolds number to 1.84×10^6 and lower during flight 1046 decreased the extent of the outboard spanwise turbulence contamination (fig. 21, planforms 3 through 6) when the calculated R_θ decreased to less than 100 over a greater portion of the outboard LETA region (fig. 22). An instrumentation error documented in the flight log probably caused the anomalous rearward transition locations indicated in figure 21 at inboard stations 16 to 19.

An interesting point noted during the Pittsburgh-based flights (for which no data are presented) involves the possibility that the supplemental anticontamination spray system is unnecessary. It was found that the leading-edge flap, designed to provide protection from insects, was sufficient by itself to protect the perforated LETA from insects without additional wetting of the leading-edge surfaces. A definitive need for the supplemental spray system for anticontamination, therefore, has not been established.

Atmospheric Ice Crystals

During flight through clouds having ice crystals, transition moved forward uniformly across the wing span, usually to about 5 percent of the chord. In all instances, laminar flow was immediately restored upon emergence from the clouds. Examples of the degree of laminar flow obtained before, during, and after entrance into an ice-crystal environment are shown in figures 23 and 24. The presence of ice crystals of sufficient magnitude and quantity to cause premature transition was consistently detected by a measurement of charging-patch current on the airplane outside the range of 0.025 to -0.05 μA. The charging patch proved very successful in the JetStar application (refs. 2 and 3) and appears to offer an inexpensive and reliable method of detecting the presence of ice crystals in flight.

Reference 3 presents a complete evaluation of the effects of clouds on the ability to obtain laminar flow and compares the experimental results with theoretical predictions. In addition, the percentage of cruise time in clouds or haze for the SAS flights was determined to be about the same (about 6 percent) as that determined in earlier statistical analyses of much more extensive USAF and NASA data (refs. 13 and 14).

Weather

The ability to cope satisfactorily with the effects of adverse weather conditions on laminar flow has

always been a factor for which insufficient information existed. The SAS tests provided encouraging results in this regard.

Early in the program, an overnight thunderstorm with a rainfall of 1.3 in. imposed a severe atmospheric test. Before takeoff on the following day (flight 1062), the test article was purged on the ground, according to standard operating procedures. The purging time, however, was not long enough to remove the unusually large quantity of accumulated water and purging was continued in climb to an altitude of 25 000 ft. At a cruise altitude of 35 000 ft and a Mach number of 0.75, measurements of the boundary-layer total-pressure deficits and the external static pressures were obviously incorrect. It was surmised that the water purged during climb above the freezing altitude was freezing on the exterior of the test article, thereby preventing attainment of laminar flow, sealing the surface static pressure taps, and clogging the total-pressure probes. The fact that full laminar flow was indicated during the following flight on the same day (table 2(a)) without any modifications to either the LETA or the instrumentation confirmed the hypothesis that icing had occurred.

This experience led to a change in procedure for flights preceded by exposure to rainfall on the ground. Standing water in the LETA was to be purged on the ground as completely as possible, and where complete purging was not completed on the ground, the PGME spray system was to be used in climb during any further purging to safeguard against icing. This procedure prevented reoccurrence of this icing problem.

The procedure was not followed completely prior to and during a later flight (flight 1138) after another exposure to an overnight rain. Complete purging of accumulated water was not accomplished on the ground and the subsequent purging during climb was not accompanied with spraying of PGME. As a result, only limited laminar flow was attained during cruise due to the formation of extensive patches of ice as water was purged. This experience reaffirmed the appropriateness of the previously recommended purging procedure.

A few flights that did not completely conform with the SAS flight-test rules were made at the beginning of the winter flights (table 2(c)) to determine the effectiveness of the anticontamination systems in protecting the leading edge from winter contaminants such as snow, ice, and runway slush and to establish some general winter operating procedures for the systems. Figure 25 is a photograph of an overnight accumulation of snow and ice on the test article and figure 26 illustrates the use of a normal hand-held deicing spray prior to takeoff for flight 1119. The test article maintained fully laminar flow during cruise for this flight, with occasional slight irregularities in the inboard region.

After another overnight exposure to light snow and temperatures of approximately 20°F, the snow was simply swept off the aircraft and wiped off the LETA with no deicing necessary before flight 1120. Fully laminar flow was attained on the test article and again during flight 1121 on the following day after an overnight exposure to temperatures near 0°F. Anomalous behavior of some of the total-pressure probes was attributed to probable probe icing during flight 1120 when the scanivalve heaters were inadvertently not operated and to a continued iced condition during flight 1121 when ambient temperatures remained well below freezing. (See table 2(c).)

Atmospheric wing icing occurred only once, during descent of flight 1122 when some ice formed on the deflected shield and on the inboard end of the notch and bump prior to use of the anti-icing fluids. Incomplete deicing of these areas resulted when the PGME supply was exhausted during a subsequent use of these systems, but ejection of secondary purge air successfully prevented ice buildup on the test article. The remaining ice on the shield and inboard of the notch and bump was manually removed before takeoff for flight 1123. Although no PGME was available for anti-icing during the flight 1123 ascent through icing conditions, fully laminar flow over the LETA was attained during cruise (table 2(c)).

Atmospheric Turbulence

It is well-known that high-frequency free-stream turbulence in wind tunnels can enter the boundary layer, grow in amplitude with downstream movement, and accelerate transition to turbulent flow. In contrast, atmospheric turbulence consists of low-frequency (gust like) disturbances which can influence transition location through changes in pressure distribution resulting from gust-induced changes in angle of attack.

Atmospheric turbulence was noted by the crew and from accelerometer measurements during cruise in flights 1081, 1090, 1133, and 1135. (See table 2.) Only in flight 1081 was there any indication of a forward transition movement. Figure 27 indicates the chordwise extent of transition was irregular over the inboard stations at t = 13:53:16, an indication of localized angle-of-attack effects. Analysis of the continuous tape data at 1-sec intervals near this time shows other irregular transition movements, but only for very short durations; these movements are also indicative of changing angle-of-attack conditions. During flights 1133 and 1135, clear-air

turbulence of $\pm 0.3g$ magnitude had no effect on the ability to maintain laminar flow. (See table 2(c).) Clear-air turbulence of $\pm 0.2g$ magnitude encountered during flight 1090 also had no effect on laminar flow (fig. 19). In figure 19, the inboard and midspan localized turbulent regions also appeared at later times when clear-air turbulence did not exist and were most likely due to insect impacts, as discussed previously. The current results suggest, therefore, that any possible adverse effects on laminar flow of atmospheric turbulence in cruise flight are probably of secondary importance.

Off-Design Conditions

Because of the possible application of LFC to short- or medium-range aircraft, which spend a significantly larger percentage of flight time during climb and descent than do long-range transports, data were taken during some flights at altitudes lower than transport cruise altitude. In particular, flights 1143, 1145, and 1146 provided significant data during descent (fig. 16). For altitudes down to about 10 000 ft, laminar flow to the front spar was attained across the span of the test article except at outboard stations 1 to 5. Premature transition at these stations was attributed previously to discontinuities caused by the hot-film sensors in this region as the unit Reynolds number increased with a decrease in altitude.

Another adverse effect of increased unit Reynolds number is the increased possibility of spanwise turbulence contamination along the attachment line. When Reynolds number exceeded about 1.6×10^6 per foot, the nominal value at cruise conditions, the momentum-thickness Reynolds number on the JetStar exceeded 95 in the inboard region, as shown in figure 22. Also, as shown in figure 11, spanwise contamination did occur for these conditions without the notch-bump leading-edge device. The device, however, protected the wing from the fuselage turbulent boundary layer to Reynolds numbers greater than 3.0×10^6 per foot (fig. 16), which correspond to attachment-line momentum-thickness Reynolds numbers significantly greater than 95. These results emphasize the need for careful consideration of leading-edge Reynolds number in the design of laminar-flow airplanes.

Calculations for the combined effects of reduced altitude (reduced angle of attack) and reduced Mach number on the theoretical chordwise pressure distributions are shown in figure 28 for various spanwise stations with the nacelle off. The pressure distributions on the upper surface at the lower altitude are even smoother and more amenable to laminar flow than those at the higher altitude, but it must be remembered that the boundary-layer flow at the larger Reynolds numbers at lower altitudes is more susceptible to transition from all external disturbances.

For some combinations of Mach number and lift coefficient, local Mach numbers on the LETA exceed a value of 1.0. When this occurs, large changes in chordwise pressure distribution may result from small changes in flight condition. A block matrix of unit Reynolds number as a function of Mach number and altitude (on which lift coefficient is dependent) is presented in figure 29. The hatched boundary is based on the local normal Mach number exceeding 1.0. Examples in figure 30 of degradation of laminar flow at inboard spanwise stations during cruise at high Mach numbers and high altitudes are consistent with this and, therefore, may be due to adverse Mach number effects.

It should be remembered that for the off-design low-altitude—reduced Mach number and high-altitude—increased Mach number conditions investigated, it was possible to attain full laminar flow without changing the suction settings used in cruise. Although the resultant suction coefficients for the off-design conditions varied, the results indicate a satisfying lack of sensitivity to suction within the test range.

Concluding Remarks

A flight-test program with a modified JetStar airplane has successfully demonstrated that (1) the leading-edge systems required for laminar-flow control (LFC) can be packaged into the volume available in a small commercial transport aircraft and (2) a perforated-surface suction approach, combined with a leading-edge flap and freezing-point-depressant spray for leading-edge anticontamination and anti-icing, is effective and practical for airline service at length Reynolds numbers at least as high as those attained during these flights. The emergence of perforated titanium as a wing surface which meets the severe aerodynamic, structural, fabrication, and operational requirements for practical aircraft applications is considered a major advance in laminar-flow technology.

Based on simulation of commercial airline-service flights, the following specific results increase the likelihood of a successful application of suction laminar-flow control to transport airplanes:

1. All LFC subsystems (suction, contamination avoidance, anti-icing, and purging) performed as intended during routine airline operational procedures.
2. No schedule delays were caused by LFC systems.

3. No pilot control of suction-system operation was required other than on-off inputs.

4. No measurable degradation of the perforated titanium suction surface occurred during 4 years of flight-testing.

5. Surface cleaning between flights was not required when the LFC systems were operated.

6. Flight through ice-crystal clouds caused loss of laminar flow, but laminar flow was restored immediately upon emergence from the clouds.

7. The percentage of cruise time that the simulated-airline-service flights were in clouds and haze (about 6 percent) was consistent with earlier statistical analysis of much more extensive USAF and NASA data.

8. A simple electrostatic "charging patch" device appears to offer an inexpensive and reliable method of detecting the presence of ice crystals in flight.

9. Flight through ice crystals appeared to provide some cleaning of the wing surface.

10. No special care was required for the suction surface and ducting when they were exposed to inclement weather on the ground or in the air (e.g., rain, snow, or icing conditions), but an operational procedure was developed for the purging of water accumulated when on the ground.

11. Snow and ice were removed on the ground with conventional equipment.

12. Possible adverse effects on laminar flow of flight through atmospheric turbulence in cruise are probably of secondary importance.

13. Appreciable periods of laminar flow were attained at altitudes as low as 10 000 ft with no adjustment to cruise suction-valve settings.

NASA Langley Research Center
Hampton, VA 23665-5225
December 14, 1989

References

1. Maddalon, D. V.; Collier, F. S., Jr.; Montoya, L. C.; and Land, C. K.: Transition Flight Experiments on a Swept Wing With Suction. AIAA-89-1893, June 1989.
2. Fisher, David F.; and Fischer, Michael C.: Development Flight Tests of JetStar LFC Leading-Edge Flight Test Experiment. *Research in Natural Laminar Flow and Laminar-Flow Control,* Jerry N. Hefner and Frances E. Sabo, compilers, NASA CP-2487, Part 1, 1987, pp. 117–140.
3. Davis, Richard E.; Maddalon, Dal V.; Wagner, Richard D.; Fisher, David F.; and Young, Ronald: *Evaluation of Cloud Detection Instruments and Performance of Laminar-Flow Leading-Edge Test Articles During NASA Leading-Edge Flight-Test Program.* NASA TP-2888, 1989.
4. Powell, Arthur G.: The Right Wing of the L.E.F.T. Airplane. *Research in Natural Laminar Flow and Laminar-Flow Control,* Jerry N. Hefner and Frances E. Sabo, compilers, NASA CP-2487, Part 1, 1987, pp. 141–161.
5. Maddalon, Dal V.; Fisher, David F.; Jennett, Lisa A.; and Fischer, Michael C.: Simulated Airline Service Experience With Laminar-Flow Control Leading-Edge Systems. *Research in Natural Laminar Flow and Laminar-Flow Control,* Jerry N. Hefner and Frances E. Sabo, compilers, NASA CP-2487, Part 1, 1987, pp. 195–218.
6. Wagner, R. D.; Maddalon, D. V.; and Fisher, D. F.: Laminar Flow Control Leading Edge Systems in Simulated Airline Service. *ICAS Proceedings 1988—16th Congress of the International Council of the Aeronautical Sciences,* Volume II, Aug. 28–Sept. 2, 1988, pp. 1014–1023. (Available as ICAS-88-3.7.4.)
7. McDonnell Douglas Corp.: *Evaluation of Laminar Flow Control Systems Concepts for Subsonic Commercial Transport Aircraft—Final Report.* NASA CR-159251, 1983.
8. Pearce, W. E.; McNay, D. E.; and Thelander, J. A.: *Laminar Flow Control Leading Edge Glove Flight Test Article Development.* NASA CR-172137, 1984.
9. Braslow, Albert L.; and Fischer, Michael C.: Design Considerations for Application of Laminar Flow Control Systems to Transport Aircraft. *Aircraft Drag Prediction and Reduction,* AGARD-R-723, July 1985, pp. 4-1–4-27.
10. Petley, Dennis H.; Alexander, William, Jr.; Wright, Andrew S., Jr.; and Vallas, Maria: *Calibration of Sonic Valves for the Laminar Flow Control, Leading-Edge Flight Test.* NASA TP-2423, 1985.
11. Gaster, M.: A Simple Device for Preventing Turbulent Contamination on Swept Leading Edges. *J. Royal Aeronaut. Soc.,* vol. 69, no. 659, Nov. 1965, pp. 788–789.
12. Pfenninger, Werner: Laminar Flow Control Laminarization. *Special Course on Concepts for Drag Reduction,* AGARD-R-654, June 1977, pp. 3-1–3-75.
13. Jasperson, William H.; Nastrom, Gregory D.; Davis, Richard E.; and Holdeman, James D.: *GASP Cloud- and Particle-Encounter Statistics, and Their Application to LFC Aircraft Studies—Volume II: Appendixes.* NASA TM-85835, 1984.
14. Jasperson, W. H.; Nastrom, G. D.; Davis, R. E.; and Holdeman, J. D.: GASP Cloud Encounter Statistics: Implications for Laminar Flow Control Flight. *J. Aircr.,* vol. 21, no. 11, Nov. 1984, pp. 851–857.

Table 1. Surface Pressure-Sensor Locations of LFC Test Article

Flute	Inboard		Center		Outboard	
	Wing station, in.	x/c	Wing station, in.	x/c	Wing station, in.	x/c
1	137.6	0.0010	169.0	0.0008	191.7	0.0006
2			169.0	.0012		
3	137.6	.0042	169.0	.0047	191.7	.0053
4			169.0	.0105		
5	137.6	.0172	169.0	.0193	191.7	.0210*
6			165.2	.0290		
7	137.6	.0350	165.2	.0400	191.7	.0450
8			165.2	.0505		
9	137.6	.0545	165.2	.0610	191.7	.0710
10			165.2	.0730		
11	137.6	.0735	165.2	.0843	191.7	.0970*
12			165.2	.0962		
13	137.6	.0930*	165.2	.1082	191.7	.1235
14			165.2	.1192		
15	137.6	.1135*	165.2	.1308*	191.7	.1502*

*Drilled orifice, 0.0135 in. diameter.

Table 2. Simulated-Airline-Service Flight Conditions and Comments

(a) Atlanta, Georgia, July 1985 (flights 1059 to 1071)

Flight	Cruise conditions			Comments
	M	$H \times 10^{-3}$, ft	$R \times 10^{-6}$, per ft	
1059	0.75	33	1.85	Laminar following initial ice-crystal encounter
	.71	37	1.50	Reduction in speed to conserve fuel; essentially 100% laminar
1060	.75	33	1.85	Laminar
	.75	37	1.62	Mostly laminar
1061	.69	29	1.90	Laminar except during ice-crystal encounter
	.72	33	1.74	Turbulent due to extended period of ice-crystal encounter*
1062	.75	35	1.74	Purging not completed on ground—continued to 25 000 ft; insect impacts near notch and bump
1063	.75	33	1.85	Laminar
1064	.75	33	1.89	Laminar
1065	.75	34	1.76	Essentially 100% laminar
1066	.75	33	1.85	Laminar
	.75	37	1.61	Laminar except at probes 13, 16, and 17; laminar at $M = 0.71$ to 0.68 during descent to 35 000 ft
1067				No data recorded
1068				No data recorded
1069	.75	33	1.84	Essentially 100% laminar with intermittent turbulence at probe 6
1070	.75	35	1.72	Essentially 100% laminar with intermittent turbulence at probe 6
1071	.75	33	1.86	Laminar

*Aircraft outside and LETA uncovered overnight during thunderstorm (1.3 in. rainfall).

Table 2. Continued

(b) Pittsburgh, Pennsylvania, September 1985 (flights 1079 to 1104)

Flight	Cruise conditions			Comments
	M	$H \times 10^{-3}$, ft	$R \times 10^{-6}$, per ft	
1079	0.75	33	1.93	Laminar except at probe 10
	.73	36	1.60	Laminar except at probes 10, 13, and 16
1080	.75	33	1.86	Laminar except at probe 10 and during ice-crystal encounter
1081	.75	33	1.85	Laminar except at $t = 13{:}53{:}16$ when clear-air turbulence ($\pm 0.1g$) encountered
1082	.75	29	2.12	Laminar but results questionable due to instrumentation discrepancies
	.75	33	1.87	Essentially 100% laminar
1083	.75	31	2.00	Laminar but some instrumentation discrepancies still present
1084	.76	35	1.80	Essentially 100% laminar with intermittent turbulence at probe 16
1085	.75	33	1.85	Laminar
1086	.75	33	1.87	Laminar; essentially laminar during descent to 27 000 ft ($R = 2.27 \times 10^6$)
1087	.75	35	1.77	Laminar except at probe 20 and during ice-crystal encounter; essentially laminar during descent to 30 000 ft ($R = 2.06 \times 10^6$)
1088	.75	33	1.89	Laminar except during ice-crystal encounter during climb from 30 000 ft; essentially laminar during descent to 27 000 ft ($R = 2.25 \times 10^6$)
1089	.75	31	2.01	Probable leaking total-pressure reference probe
1090	.75	28	2.28	Laminar except at probes 9, 17, and 18; clear-air turbulence ($\pm 0.2g$) encountered; during climb to 32 000 ft, $M = 0.76$ ($R = 2.23$ to 1.90), turbulence at probes 9, 17, 18 dissipates
	.75	33	1.87	Laminar except at probe 9; during descent to 24 000 ft ($R = 2.20 \times 10^6$), turbulence at probes 9 and 17 redevelops; 0.015-in. insect measured inboard near L.E. after flight
1091	.75	33	1.88	Essentially 100% laminar; essentially 100% laminar during descent to 27 000 ft ($R = 2.35 \times 10^6$); turbulence at probe 4; <0.015-in. insect measured inboard near L.E. after flight
1092	.75	31	2.05	Laminar except at probe 16; 0.006-in. insect measured between probes 16 and 17 at $x/c \approx 0.02$
1093	.75	31	2.04	Laminar except during descent to 25 000 ft
1094	.75	33	1.90	Laminar except during ice-crystal encounter
1095	.75	37	1.70	Laminar except at probes 13, 15, and 16
1096	.75	31	2.09	Laminar; laminar during descent to 28 000 ft
1097	.75	31	2.05	Essentially 100% laminar except during ice-crystal encounter; laminar during descent to 25 000 ft
1098	.76	35	1.86	Laminar
1099	.75	35	1.76	Laminar except during ice-crystal encounter
1100	.75	33	1.90	Laminar except during ice-crystal encounter
	.75	37	1.68	Climb to top of cirrus reestablished laminar
1101	.75	35	1.75	Essentially 100% laminar
1102	.75	35	1.75	Laminar; encountered jet exhaust from several aircraft while taxiing with no detrimental effect on laminar flow during flight
1103	.75	35	1.73	Essentially 100% laminar; inclement weather with thunderstorms; icing on notch and bump during descent
1104	.75	35	1.73	Exhausted remaining PGME during climbout at 6000 ft; in clouds from 25 000 ft to 33 000 ft, caused probes to accumulate ice

Table 2. Continued

(c) Cleveland, Ohio, January and February 1986 (flights 1116 to 1153)

Flight	Cruise conditions			Comments
	M	$H \times 10^{-3}$, ft	$R \times 10^{-6}$, per ft	
1116†	0.75	37	1.71	Essentially 100% laminar except at probes 13, 16, and 17
1117†	.75	33	2.00	Laminar
	.73	37	1.69	Laminar with some irregularity inboard
1118†	.75	33	2.02	Laminar except during ice-crystal encounter
1119†	.75	35	1.75	Essentially 100% laminar; aircraft deiced 25 minutes prior to takeoff after overnight exposure to light snow and icing; low-altitude cruise in icing conditions at 7000 ft did not produce ice on LETA
1120†	.75	29	2.25	Instrumentation discrepancies most likely due to probe icing (scanivalve heaters inadvertently not turned on); light snow wiped off LETA before takeoff without deicing; packed snow on runway during landing
1121†	.75	31	1.89	Laminar except at probes 1 and 4, which register numbers indicative of probe icing; overnight temperatures near 0°F
1122	.75	33	1.95	Laminar except at probes 1, 2, 3, 17, and 18; LETA covered with white film (salt or ice) approx 0.001 to 0.002 in. thick; PGME supply exhausted during descent
1123	.75	31	2.08	Laminar; Cleveland taxiways wet from melting snow; no PGME available
1131	.75	33	1.91	Mostly turbulent due to ice-crystal environment
	.75	37	1.65	Mostly turbulent due to ice-crystal environment
1132	.76	33	1.92	Mostly turbulent due to ice-crystal environment
	.75	37	1.65	Continued cirrus formations prevent laminar flow
1133	.75	33	1.91	Essentially 100% laminar; clear-air turbulence ($\pm 0.3g$) encountered; essentially 100% laminar during descent to 17 000 ft ($R = 2.62 \times 10^6$) except at probe 4
1134	.76	28	2.35	Mostly turbulent likely due to deteriorated condition of notch and bump; extensive repairs to notch and bump prior to flight due to raised edges and blistering
1135	.75	33	1.91	Essentially 100% laminar except during ice-crystal encounters; clear-air turbulence ($\pm 0.3g$) encountered
1136	.76	33	1.92	Essentially 100% laminar except for occasional turbulence at midspan

†Not completely in conformance with SAS flight-test rules.

Table 2. Concluded

(c) Concluded

Flight	Cruise conditions			Comments
	M	$H \times 10^{-3}$, ft	$R \times 10^{-6}$, per ft	
1137	0.75	33	1.98	Turbulent likely due to poor notch and bump condition; laminar at lower R; prior to takeoff, LETA deiced (approx 0.25 in. ice buildup after overnight freezing rain); some ice patches may have reformed before takeoff as suggested by incongruous measurements by probe 2 and static-pressure taps 6 and 8; a set parking brake caused tires to blow on landing
1138	.76	35	1.87	Laminar limited by ice patches on LETA resulting from faulty purge procedures
1139	.75	33	1.97	Essentially 100% laminar; essentially 100% laminar during descent to at least 21 000 ft ($R = 2.55 \times 10^6$)
1140	.76	35	1.78	Laminar
1141	.76	35	1.77	Laminar
	.74	36	1.66	Laminar except for small disturbance at probe 16
1142	.76	33	2.01	Laminar
1143	.76	35	1.80	Laminar; essentially 100% laminar during descent to 10 000 ft ($R = 2.88 \times 10^6$)
1144	.75	33	2.01	Essentially 100% laminar; essentially 100% laminar during descent to 15 000 ft ($R = 2.74 \times 10^6$)
1145	.75	35	1.80	Laminar except for occasional small disturbance at probe 16
1146	.76	33	2.04	Essentially 100% laminar
	.76	37	1.64	Essentially 100% laminar except for turbulence at probes 13 and 16; essentially 100% laminar during descent to 12 600 ft ($R = 3.20 \times 10^6$)
1147	.75	35	1.75	Essentially 100% laminar; essentially 100% laminar during descent to 10 000 ft ($R = 2.8 \times 10^6$)
1148	.75	34	1.85	Laminar; turbulent during ice-crystal encounters during climb and descent below 32 000 ft
1149	.75	33	1.94	Laminar; 2 in. of snow accumulated on LETA overnight brushed off before takeoff and LETA deiced with glycol
1150	.75	35	1.76	Laminar; turbulence at probe 4 during descent at 22 000 ft
1151	.75	35	1.74	Essentially 100% laminar except for intermittent turbulence at probe 16
1152	.75	31	2.10	Laminar
1153	.75	35	1.80	Essentially 100% laminar except for intermittent turbulence at probe 16
	.75	39	1.48	Essentially 100% laminar except for intermittent turbulence at probes 11 to 16

Table 3. Weather Conditions for Simulated-Airline-Service City Pairs

(a) Atlanta, Georgia

Flight	Date	Origin	Weather	Destination	Weather
1059	07-15-85	Edwards, CA	T=75°F, High clouds	Amarillo, TX	T=77°F, Sunny
1060	07-15-85	Amarillo, TX	T=77°F, Sunny	Barksdale, LA	T=91°F, Scattered clouds
1061	07-15-85	Barksdale, LA	T=91°F, Scattered clouds	Atlanta, GA	
1062	07-16-85	Atlanta, GA		St. Louis, MO	Sunny, warm
1063	07-16-85	St. Louis, MO	Sunny, warm	Atlanta, GA	Thunderstorms
1064	07-17-85	Atlanta, GA	T=77°F, Clear	Cleveland, OH	T=72°F, Scattered clouds
1065	07-17-85	Cleveland, OH	T=72°F, Scattered clouds	Springfield, MO	T=80°F, Clear
1066	07-17-85	Springfield, MO	T=80°F, Clear	Atlanta, GA	T=75°F, Overcast
1067	07-18-85	Atlanta, GA		New Orleans, LA	
1068	07-18-85	New Orleans, LA		Atlanta, GA	
1069	07-20-85	Atlanta, GA	T=85°F, Hazy sunshine	Norfolk, VA	T=82°F, Very hazy
1070	07-20-85	Norfolk, VA	T=88°F, Very hazy	Atlanta, GA	T=85°F, Hazy overcast
1071	07-22-85	Atlanta, GA	T=85°F, Hazy overcast	Langley Field, VA	T=87°F, Hazy overcast

(b) Pittsburgh, Pennsylvania

Flight	Date	Origin	Weather	Destination	Weather
1079	09-09-85	Edwards, CA	T=60°F, Clear	Denver, CO	T=59°F
1080	09-09-85	Denver, CO	T=63°F	St. Louis, MO	T=88°F
1081	09-09-85	St. Louis, MO	T=90°F	Pittsburgh, PA	T=80°F
1082	09-10-85	Pittsburgh, PA	T=80°F, Broken clouds	Boston, MA	T=63°F, Overcast
1083	09-10-85	Boston, MA	T=63°F, Overcast	Pittsburgh, PA	T=76°F, Overcast
1084	09-11-85	Pittsburgh, PA	T=61°F, Scattered clouds	Chicago, IL	T=63°F, Scattered clouds
1085	09-11-85	Chicago, IL	T=65°F, Scattered clouds	Chattanooga, TN	T=83°F, Broken clouds
1086	09-11-85	Chattanooga, TN	T=85°F, Scattered clouds	Pittsburgh, PA	T=69°F, Scattered clouds
1087	09-12-85	Pittsburgh, PA	T=46°F, Clear	Nashville, TN	T=67°F
1088	09-12-85	Nashville, TN	T=71°F, Clear	Cleveland, OH	T=58°F, Broken clouds
1089	09-12-85	Cleveland, OH	T=59°F, Broken overcast	Pittsburgh, PA	T=60°F, Clear
1090	09-13-85	Pittsburgh, PA	T=47°F	Charleston, SC	T=69°F, Scattered clouds
1091	09-13-85	Charleston, SC	T=70°F	Washington-Dulles	T=62°F, Scattered clouds
1092	09-13-85	Washington-Dulles		Pittsburgh, PA	T=60°F, Scattered clouds
1093	09-14-85	Pittsburgh, PA	T=50°F	Detroit, MI	T=55°F, Clear
1094	09-14-85	Detroit, MI	T=60°F, Mostly clear	Pittsburgh, PA	T=60°F, Scattered clouds
1095	09-16-85	Pittsburgh, PA	T=50°F	Bangor, ME	T=70°F
1096	09-16-85	Bangor, ME	T=69°F	New York-Kennedy	T=75°F
1097	09-16-85	New York-Kennedy	T=75°F	Raleigh-Durham	T=75°F, Thin broken clouds
1098	09-16-85	Raleigh-Durham	T=75°F	Pittsburgh, PA	T=72°F, Thin scattered clouds
1099	09-17-85	Pittsburgh, PA	T=52°F	Kalamazoo, MI	T=65°F, Broken clouds
1100	09-17-85	Kalamazoo, MI	T=74°F, Broken clouds	Pittsburgh, PA	T=76°F, Broken clouds
1101	09-18-85	Pittsburgh, PA	T=56°F	St. Louis, MO	T=72°F, Clear
1102	09-18-85	St. Louis, MO	T=76°F, Clear but hazy	Oklahoma City, OK	T=79°F, Scattered clouds
1103	09-18-85	Oklahoma City, OK	T=82°F, Overcast	Albuquerque, NM	T=66°F, Broken clouds
1104	09-18-85	Albuquerque, NM	T=68°F, Broken clouds	Edwards, CA	T=67°F

Table 3. Concluded

(c) Cleveland, Ohio

Flight	Date	Origin	Weather	Destination	Weather
1116	01-13-86	Edwards, CA	T=29°F, Clear	Amarillo, TX	T=52°F, Clear
1117	01-13-86	Amarillo, TX	T=55°F, Clear	Springfield, IL	T=28°F, Hazy
1118	01-13-86	Springfield, IL	T=27°F, Overcast	Cleveland, OH	T=18°F, Overcast, snow on ground
1119	01-14-86	Cleveland, OH	T=20°F, Light snow	Cleveland, OH	T=18°F, Light snow
1120	01-14-86	Cleveland, OH	T=22°F, Light snow	Cleveland, OH	Snow
1121	01-15-86	Cleveland, OH	T=12°F, Thin scattered clouds	Cleveland, OH	
1122	01-16-86	Cleveland, OH	T=32°F, Clear	Syracuse, NY	T=22°F, Overcast
1123	01-16-86	Syracuse, NY	T=26°F, Overcast	Cleveland, OH	T=45°F, Thin overcast
1131	02-19-86	Edwards, CA	T=57°F, Sprinkling	Amarillo, TX	T=64°F, Overcast
1132	02-19-86	Amarillo, TX	T=64°F, Overcast	Springfield, IL	T=37°F, Fog
1133	02-19-86	Springfield, IL	T=38°F, Overcast, fog	Cleveland, OH	T=35°F, Fog
1134	02-20-86	Cleveland, OH	T=35°F, Overcast	Atlanta, GA	T=66°F, Scattered clouds
1135	02-20-86	Atlanta, GA	T=69°F, Hazy	Atlantic City, NJ	T=42°F, Fog
1136	02-20-86	Atlantic City, NJ	T=42°F, Overcast	Cleveland, OH	T=46°F, Overcast, fog
1137	02-21-86	Cleveland, OH	T=27°F, Snowing	Boston, MA	T=37°F, Light rain
1138	02-22-86	Boston, MA	T=36°F, Clear	Cleveland, OH	T=28°F, Broken clouds
1139	02-24-86	Cleveland, OH	T=26°F, Overcast	Knoxville, TN	T=41°F, Raining
1140	02-24-86	Knoxville, TN	T=41°F, Raining	Tampa, FL	T=70°F, Scattered clouds
1141	02-24-86	Tampa, FL	T=70°F, Scattered clouds	Nashville, TN	T=40°F, Overcast
1142	02-24-86	Nashville, TN	T=40°F, Overcast	Cleveland, OH	T=19°F, Light frost
1143	02-25-86	Cleveland, OH	T=22°F, Clear	Green Bay, WI	T=16°F, Broken clouds
1144	02-25-86	Green Bay, WI	T=21°F, Thin overcast	Louisville, KY	T=35°F, Scattered clouds
1145	02-25-86	Louisville, KY	T=35°F, Hazy	Cleveland, OH	T=27°F, Scattered clouds
1146	02-26-86	Cleveland, OH	T=24°F, Overcast	Burlington, VT	T=02°F, Light snow
1147	02-26-86	Burlington, VT	T=02°F, Clear	Langley Field, VA	T=38°F, High scattered clouds
1148	02-26-86	Langley Field, VA	T=39°F, High scattered clouds	Cleveland, OH	T=32°F, Light snow
1149	02-27-86	Cleveland, OH	T=12°F, Partly cloudy	Richmond, VA	T=32°F, Light snow
1150	02-27-86	Richmond, VA	T=35°F, Overcast	Cleveland, OH	T=18°F, Clear
1151	02-28-86	Cleveland, OH	T=09°F, Light snow	Des Moines, IA	T=19°F, Clear
1152	02-28-86	Des Moines, IA	T=22°F, Clear	Denver, CO	T=46°F, Clear
1153	02-28-86	Denver, CO	T=54°F	Edwards, CA	T=76°F, Clear

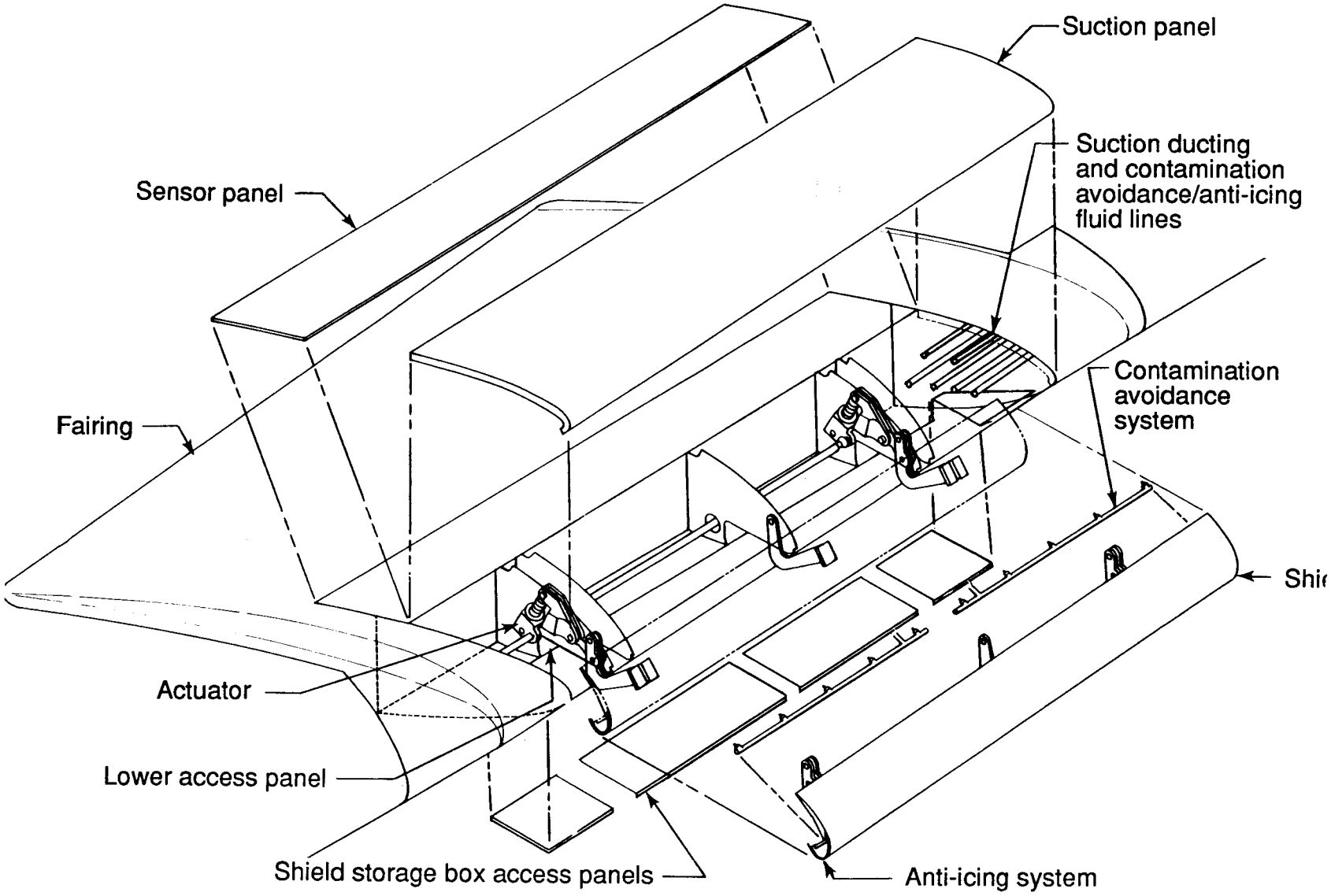

Figure 1. Exploded view of principal components of perforated-surface leading-edge test article.

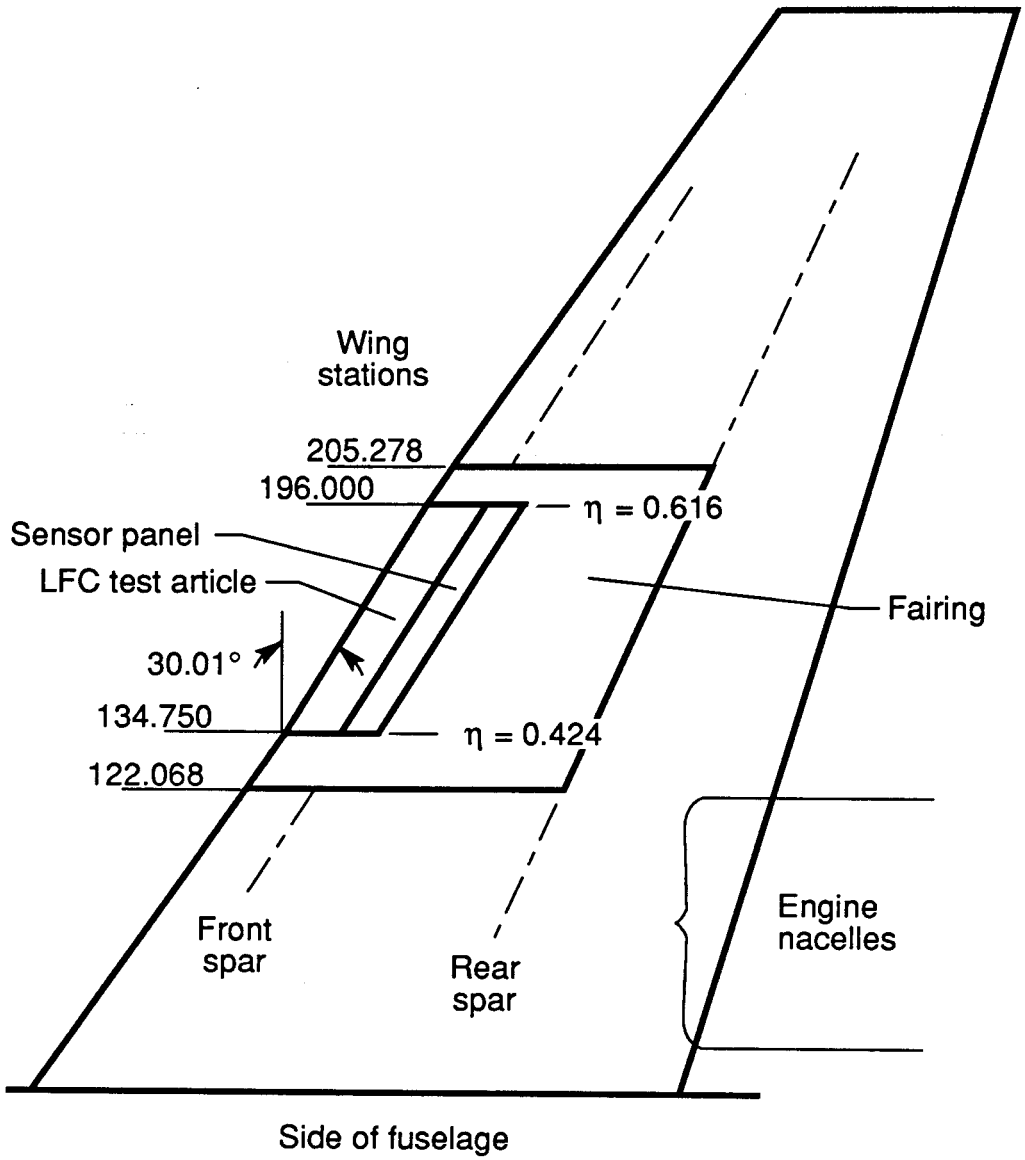

Figure 2. Planform of leading-edge test article. Dimensions in inches unless otherwise indicated.

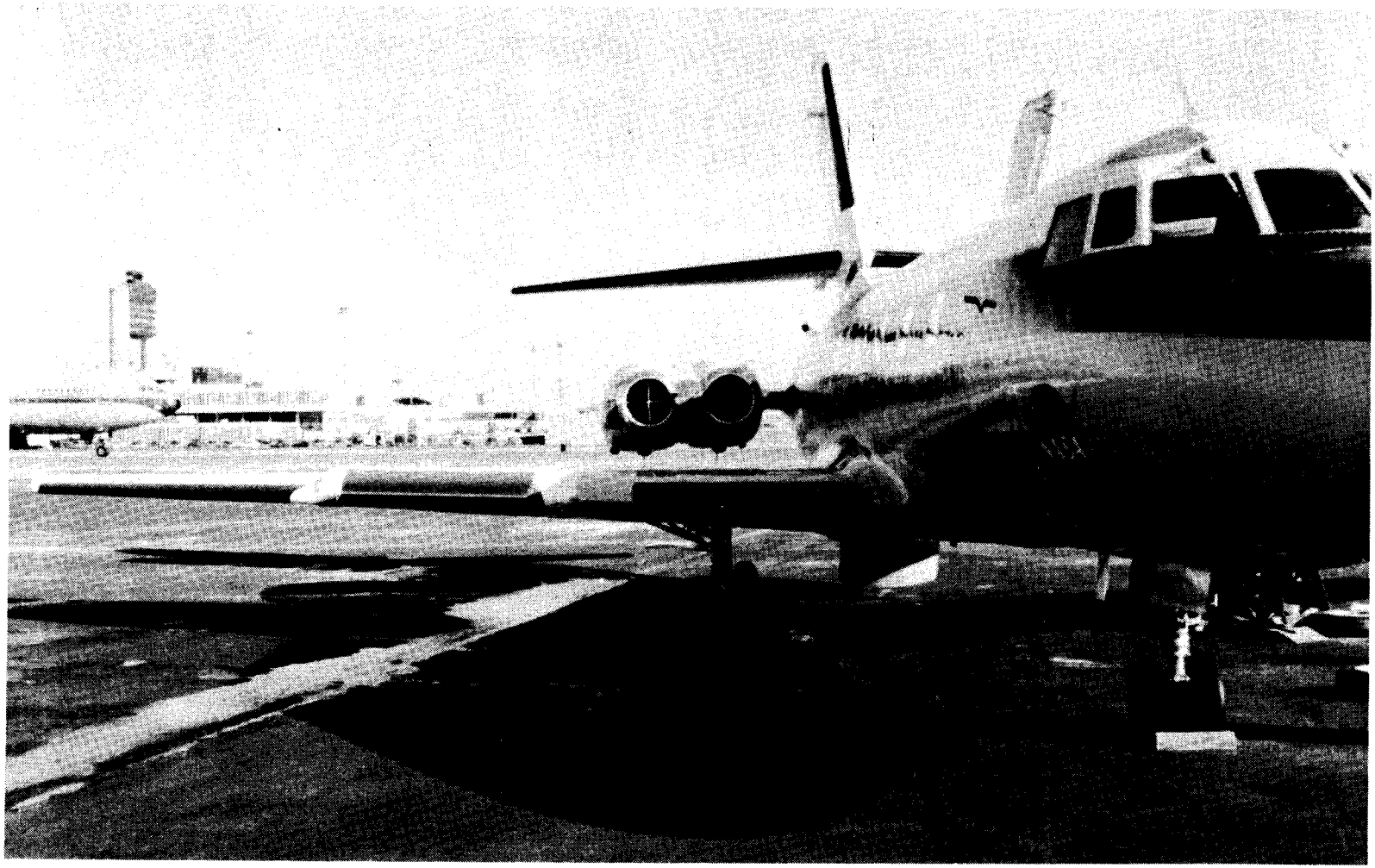

L-89-151

Figure 3. NASA JetStar airplane.

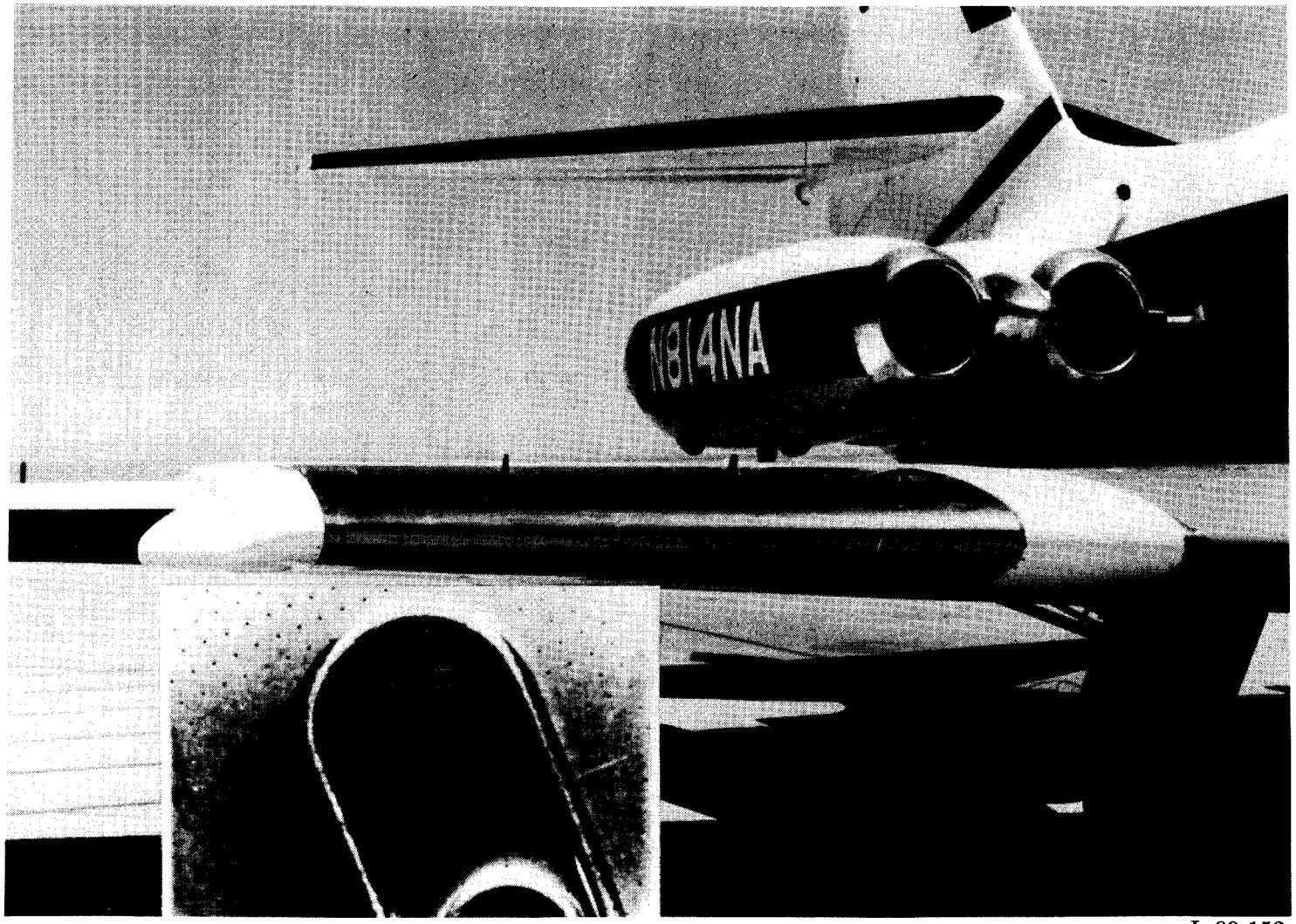

L-89-152

Figure 4. Closeup view of perforated-surface leading-edge test article on JetStar airplane with flap retracted.

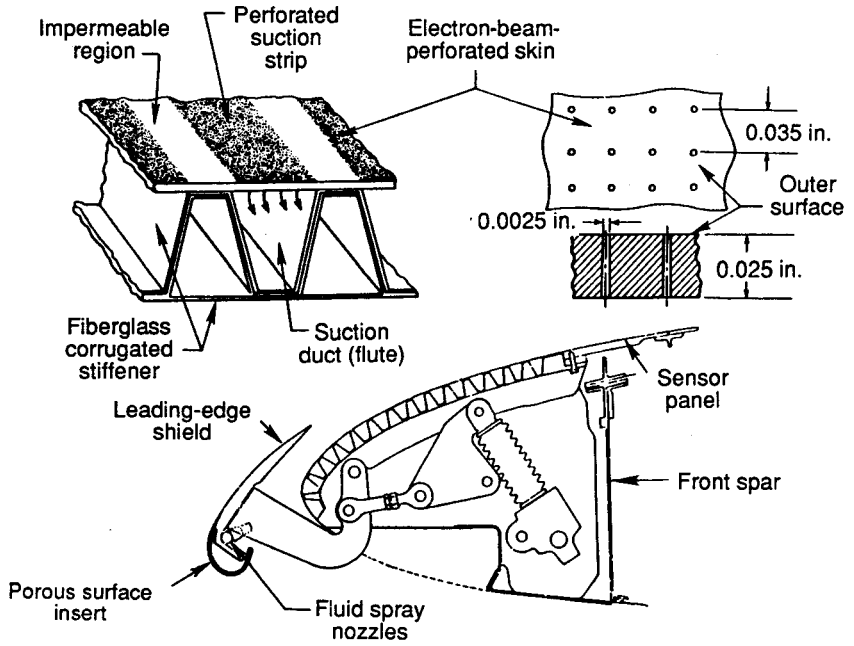

Figure 5. Cross sections of perforated-surface leading-edge test article.

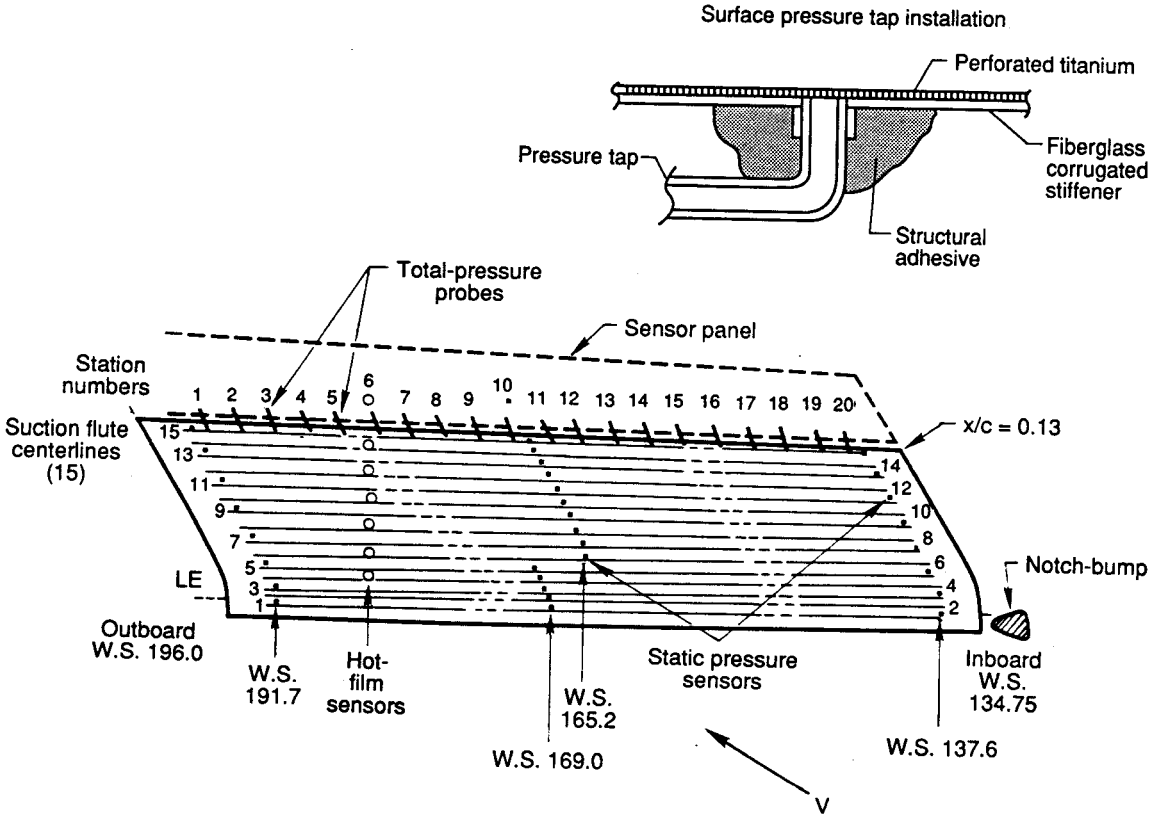

Figure 6. Perforated-surface instrumentation. Wing spanwise stations are in inches.

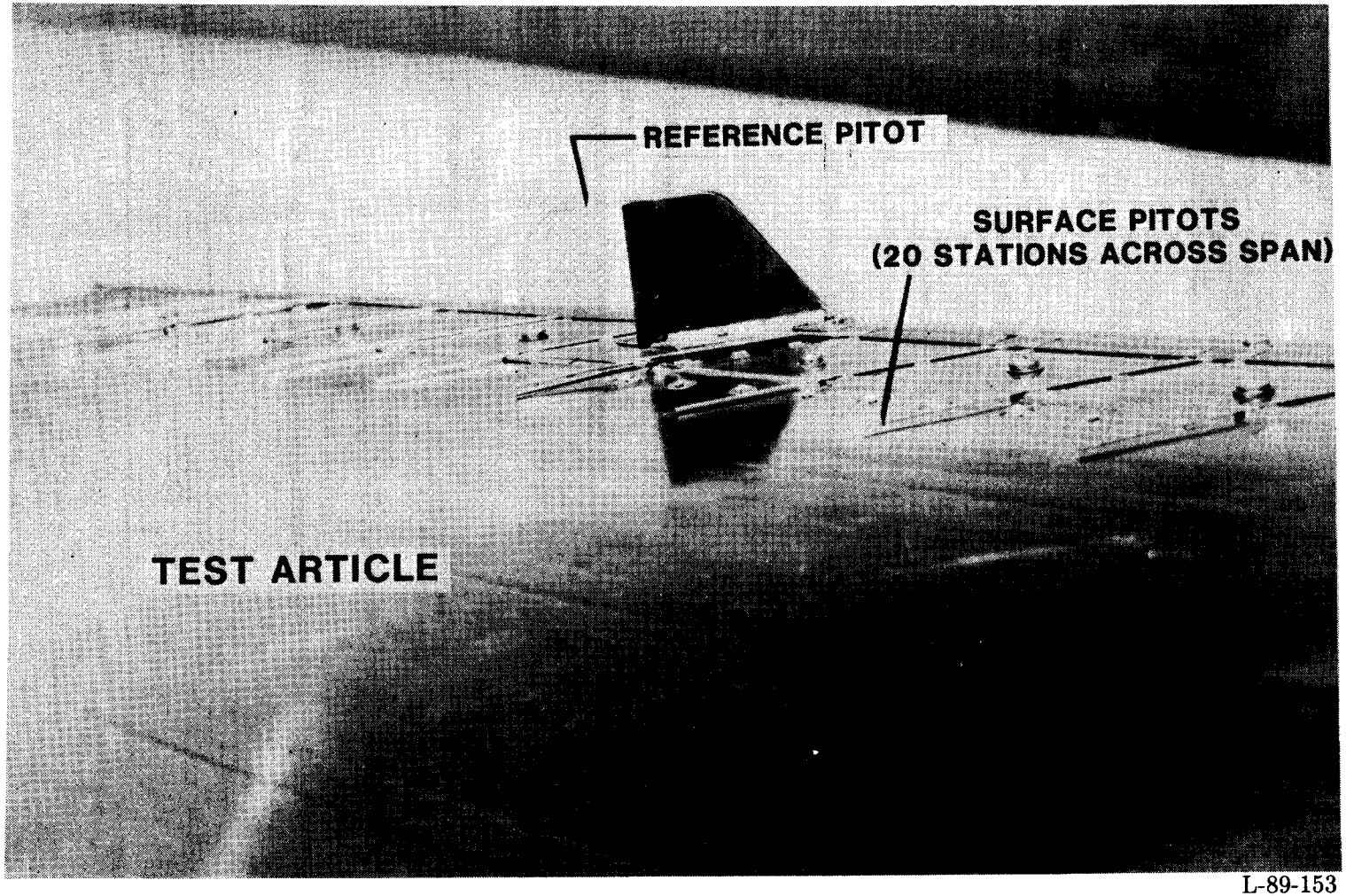

L-89-153

Figure 7. Instrumentation for monitoring condition of boundary layer.

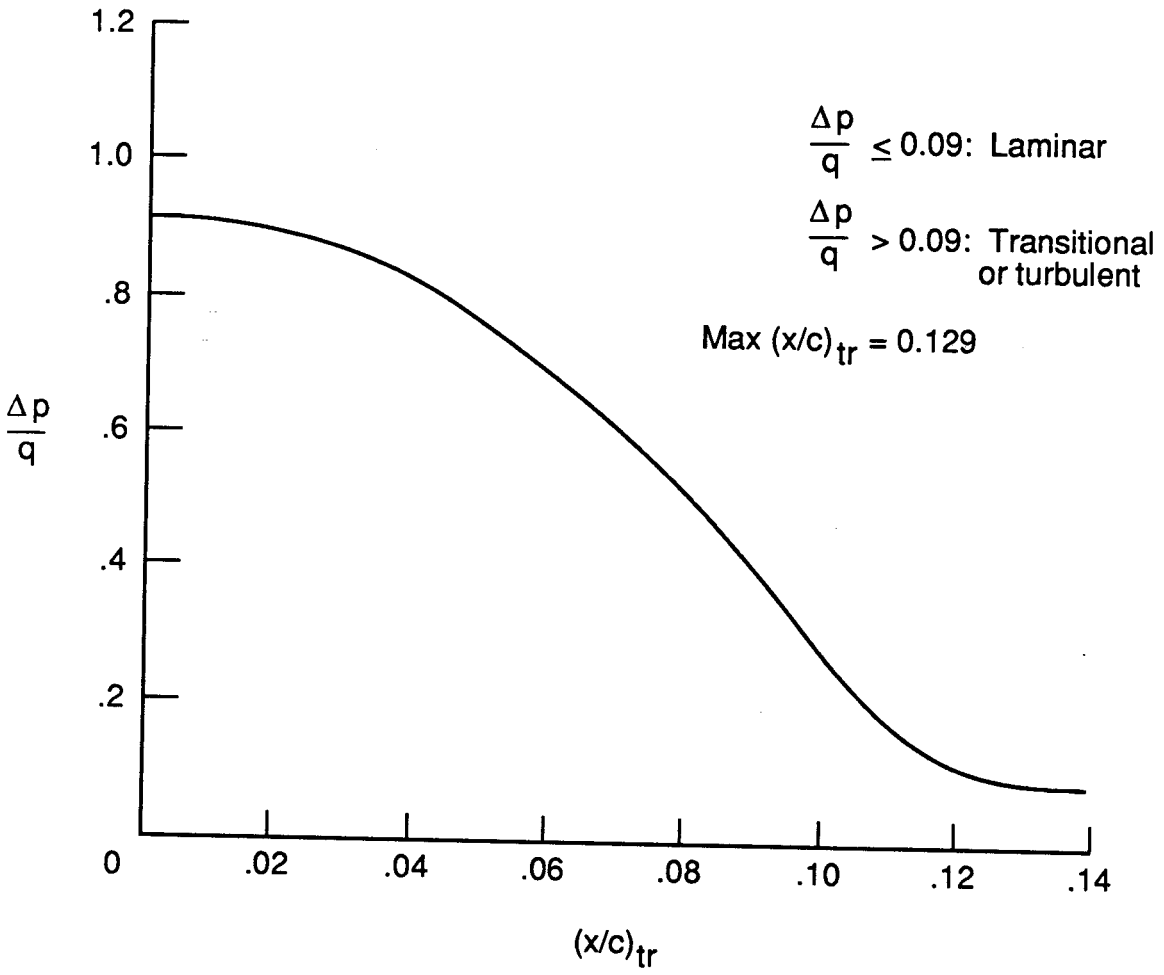

Figure 8. Calibration of total-pressure differentials at leading-edge test article trailing edge with transition position. $M = 0.75$; $H = 36\,000$ ft.

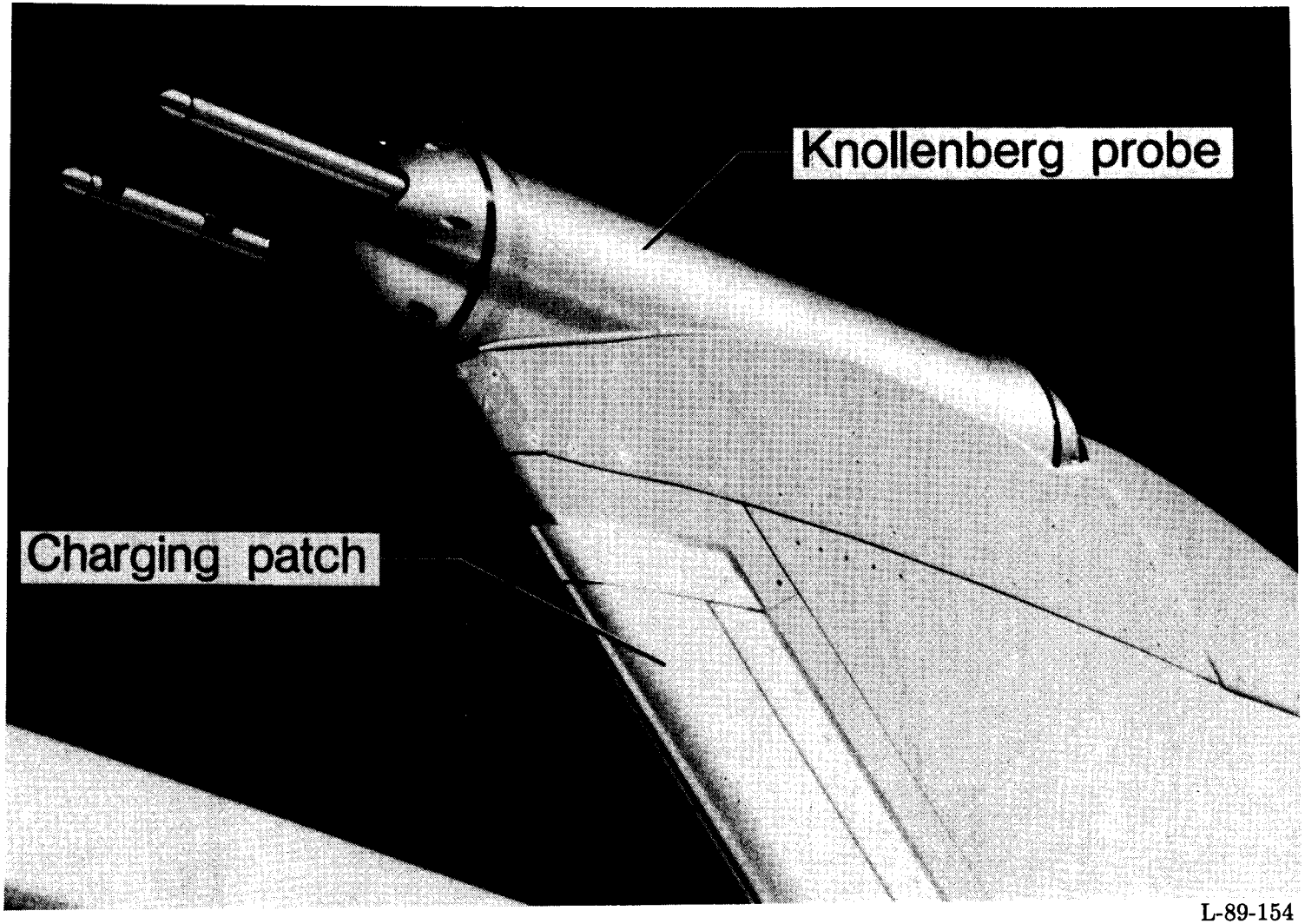

L-89-154

Figure 9. Laser particle spectrometer (Knollenberg probe).

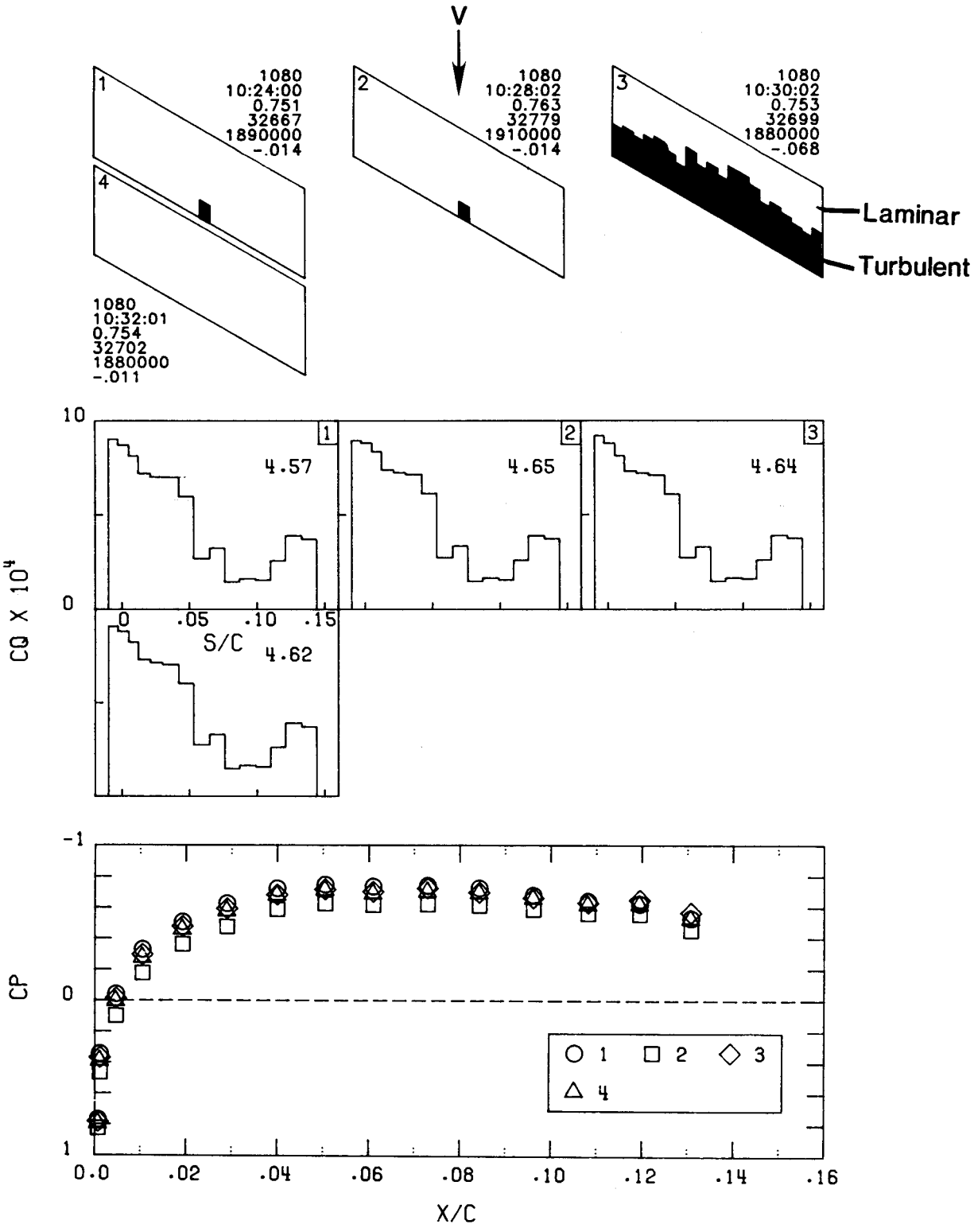

Figure 10. Representative data snapshot for flight 1080.

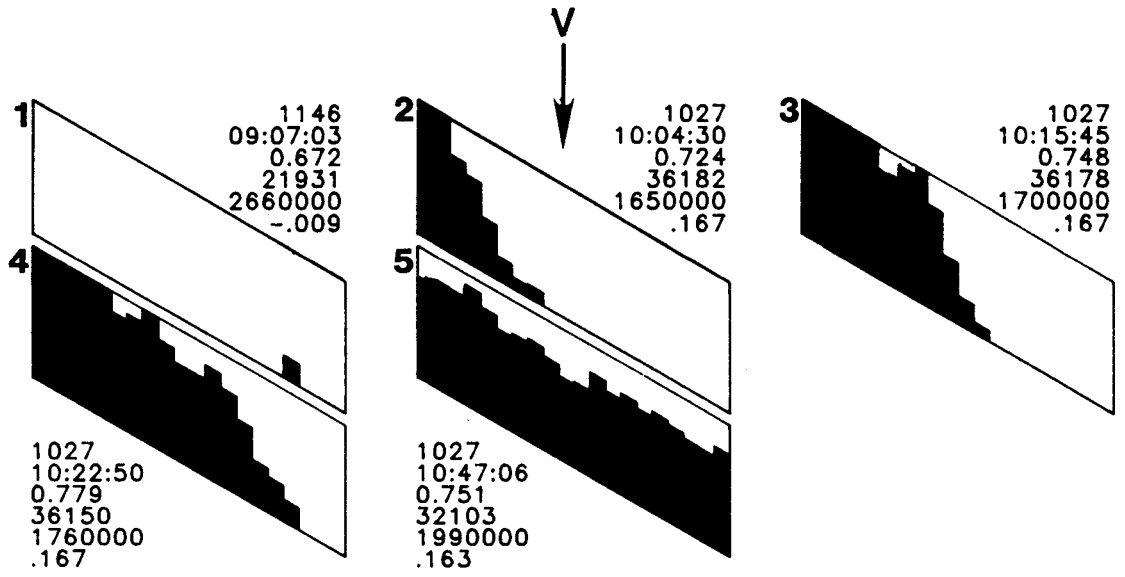

Figure 11. Effect of unit Reynolds number on spanwise turbulence contamination for flight 1027 without notch and bump and flight 1146 with notch and bump.

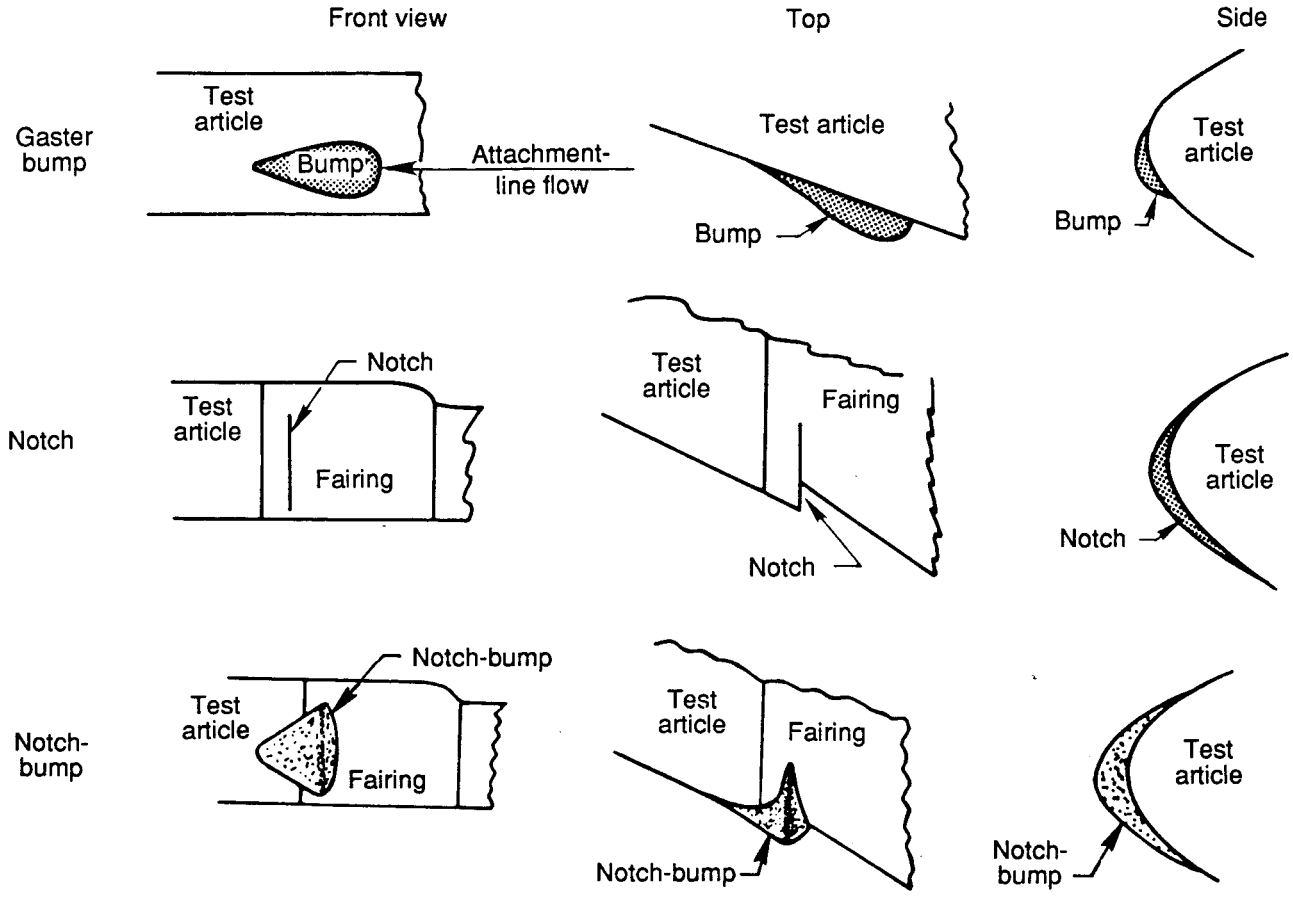

Figure 12. Candidate methods to control spanwise turbulence contamination.

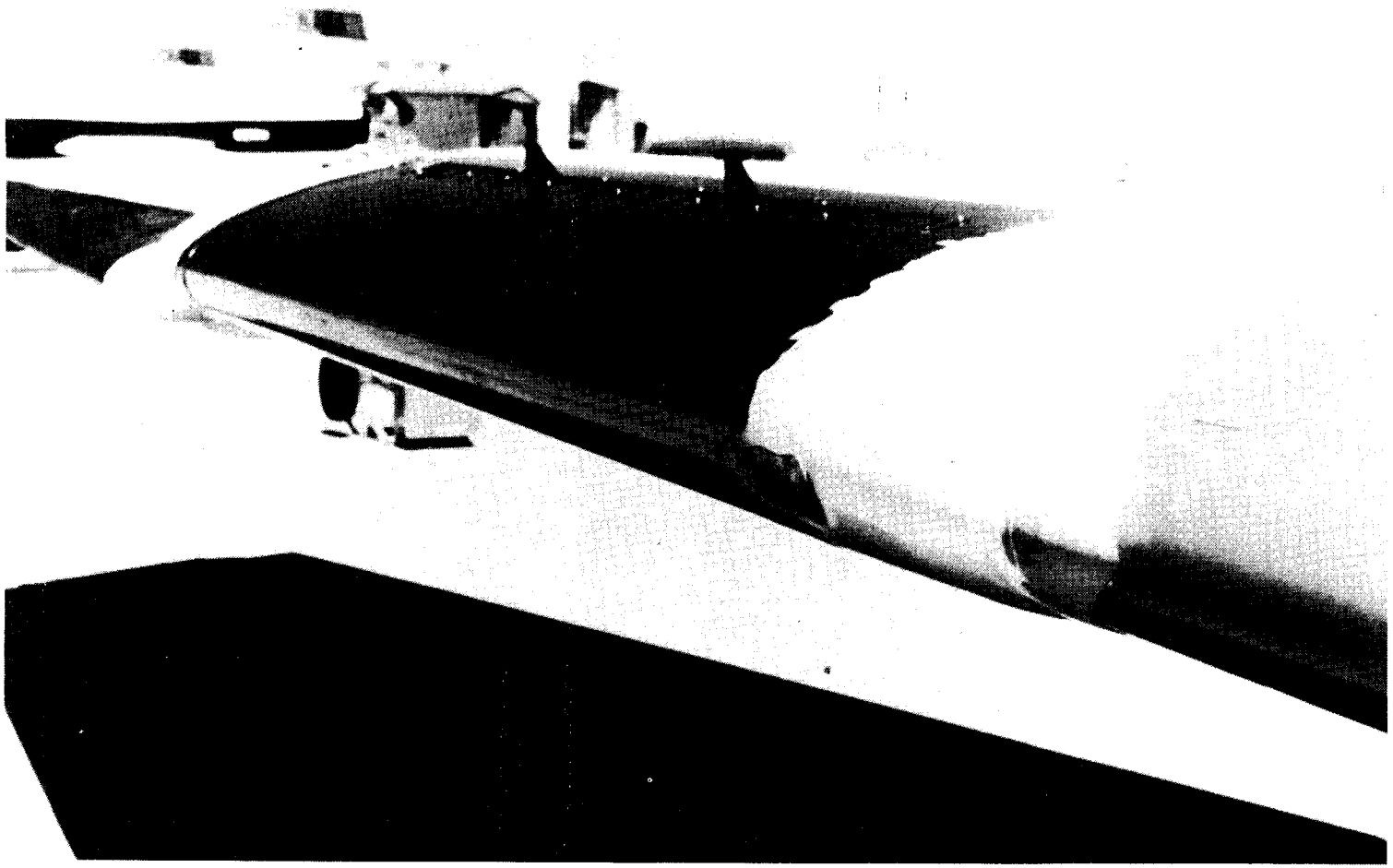

L-88-5402

Figure 13. Leading-edge notch-bump configuration selected for control of spanwise turbulence contamination.

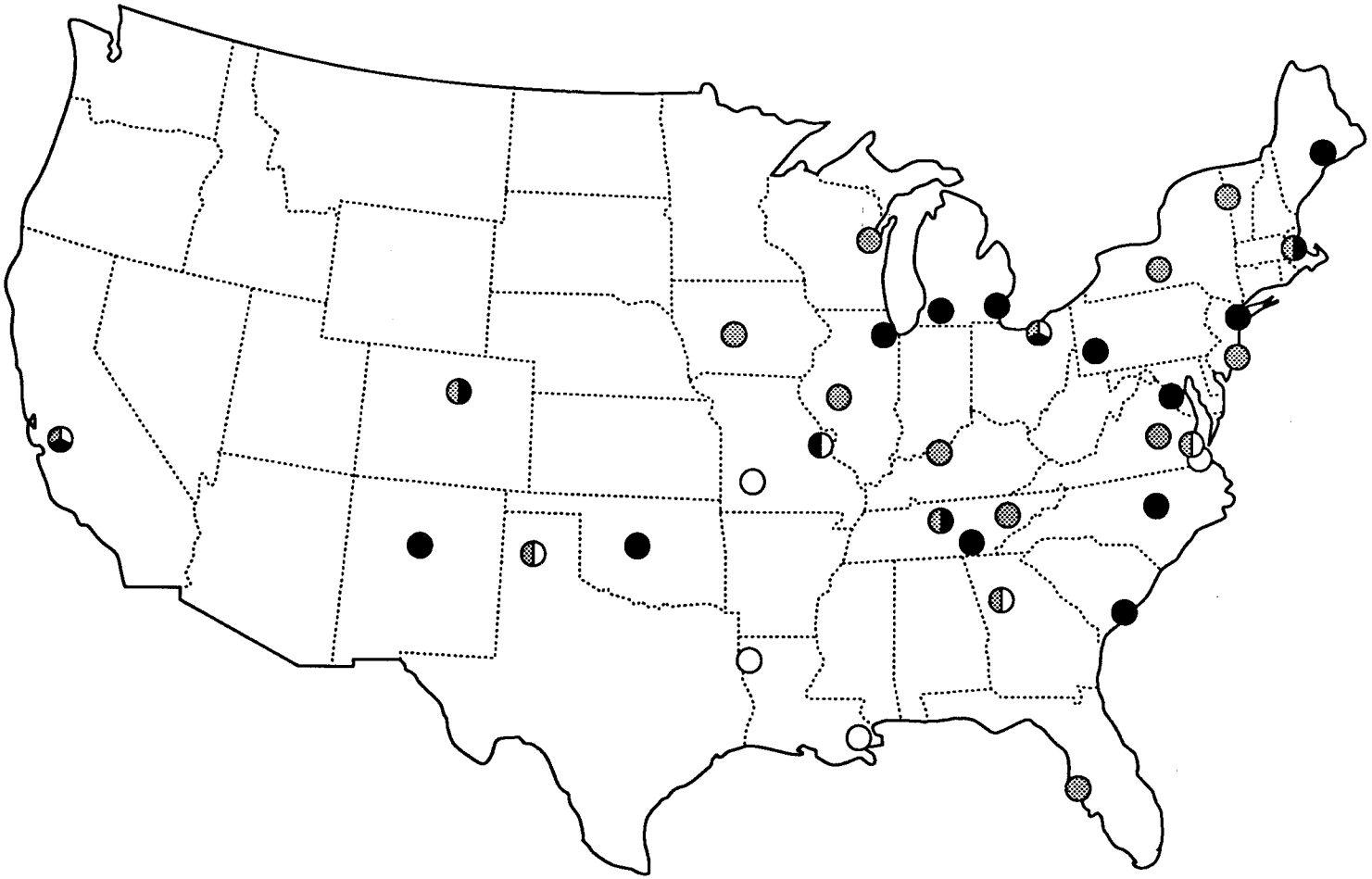

Figure 14. Simulated-airline-service flights.

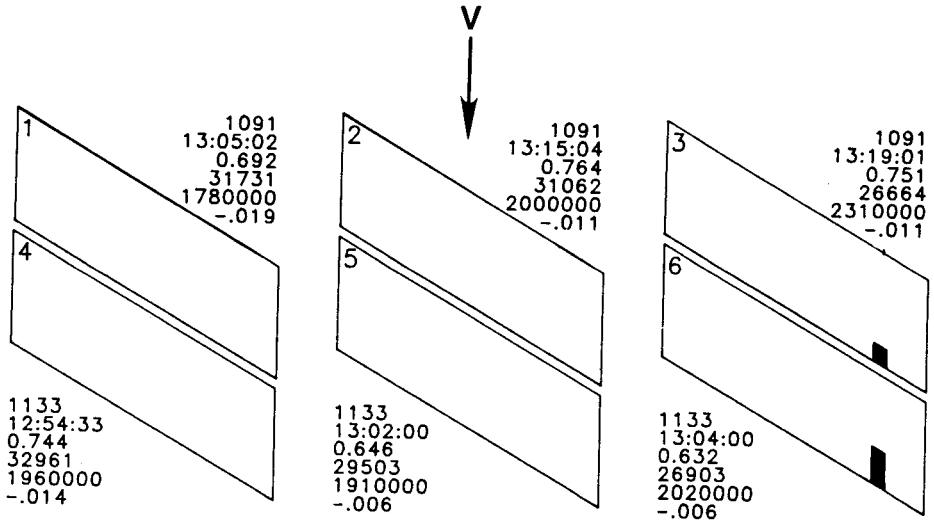

Figure 15. Effect of uneven hot-film sensor for flights 1091 and 1133.

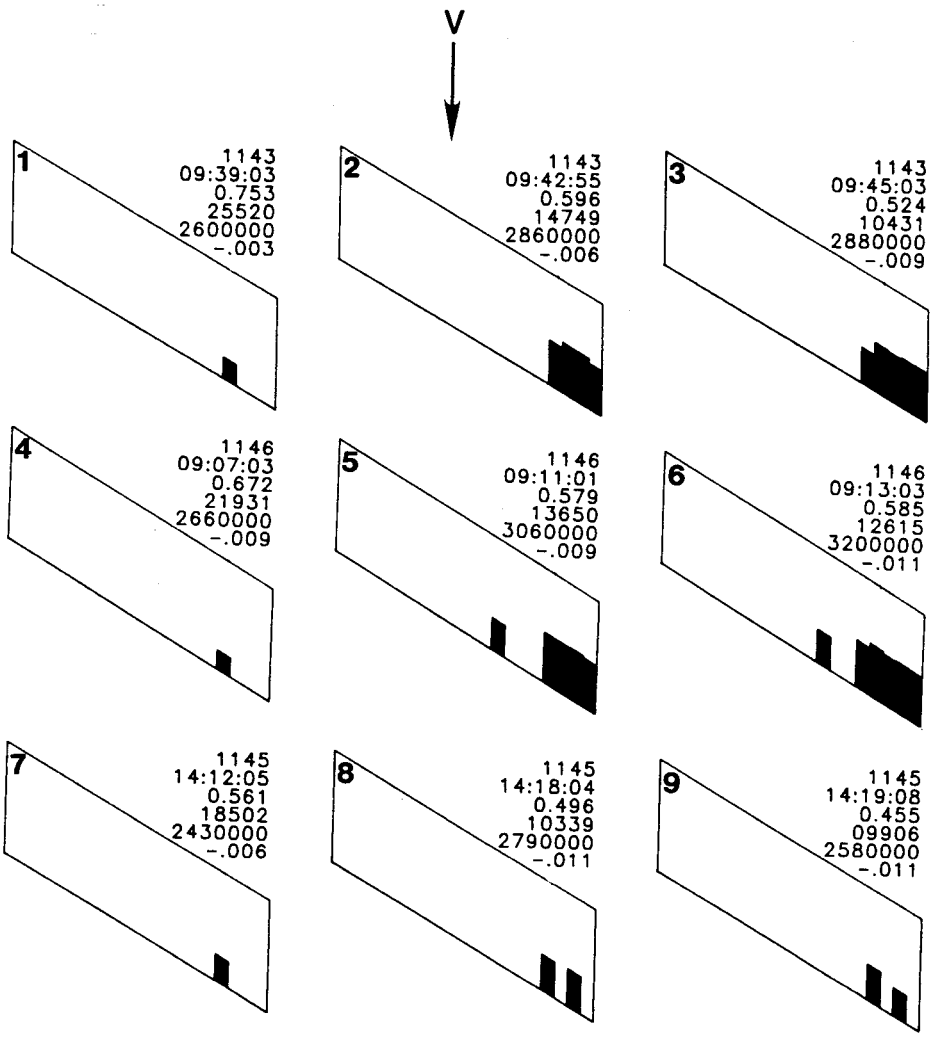

Figure 16. Off-design effects for flights 1143, 1145, and 1146 at lower than cruise altitudes.

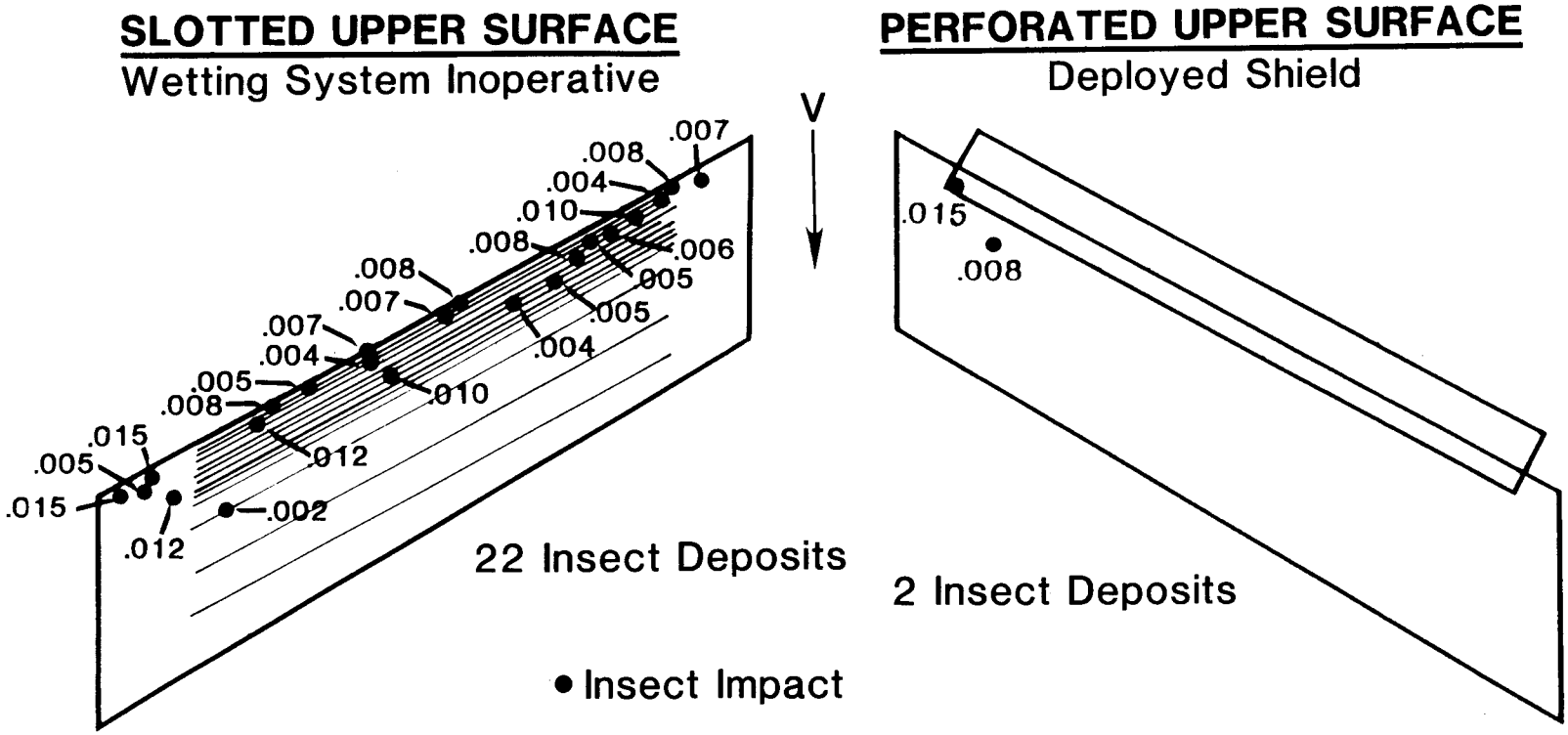

Figure 17. Effectiveness of anticontamination shield for flight 1083. Height of insect deposits given in inches.

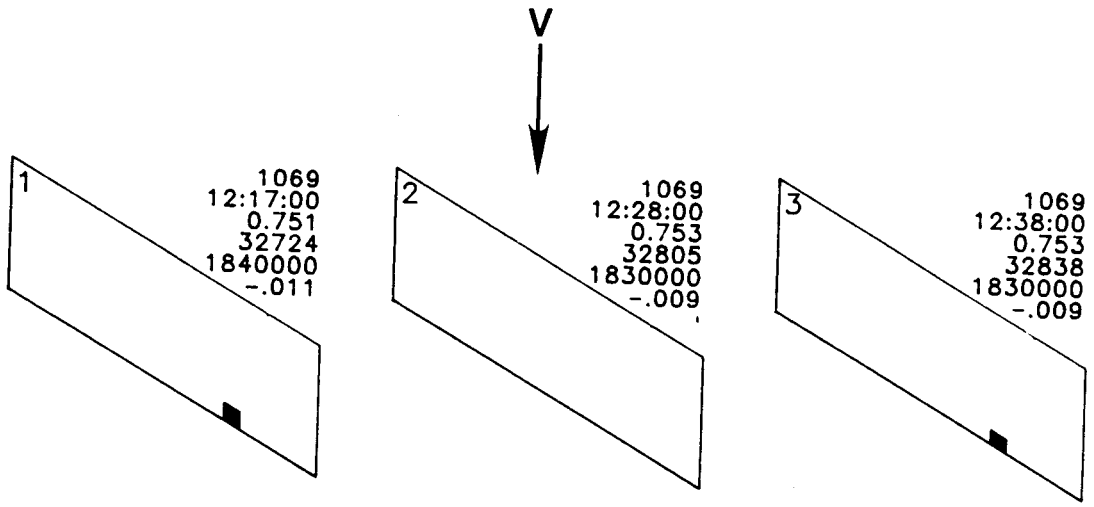

Figure 18. Effect of probable insect impact during flight 1068 as evidenced during flight 1069.

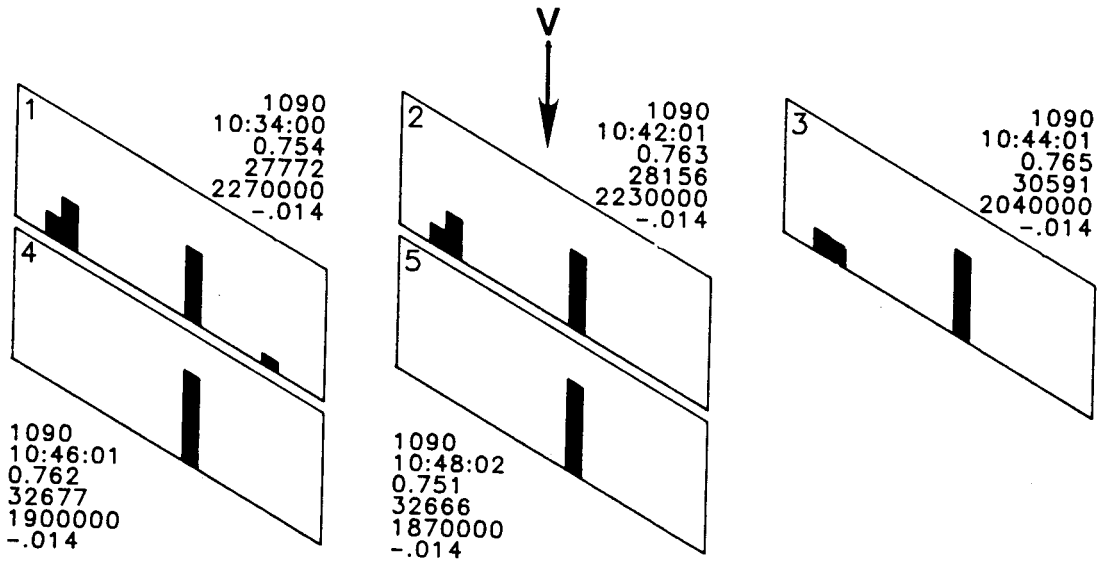

Figure 19. Data for flight 1090 with an insect impact during light clear-air turbulence; free-stream turbulence of $\pm 0.2g$ for planforms 1 and 4.

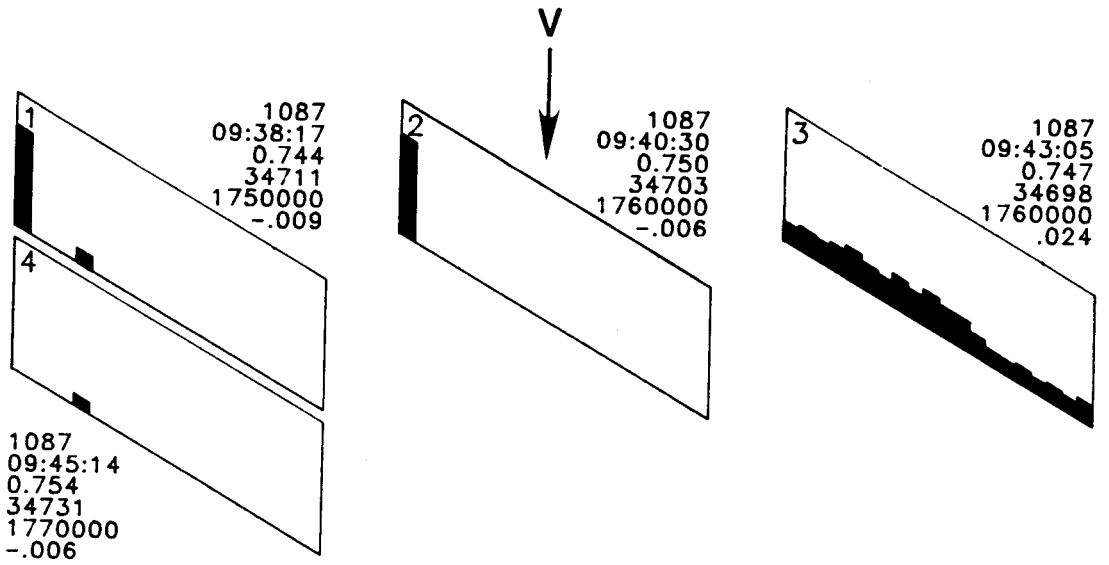

Figure 20. Effect of atmospheric ice crystals on insect residue for flight 1087.

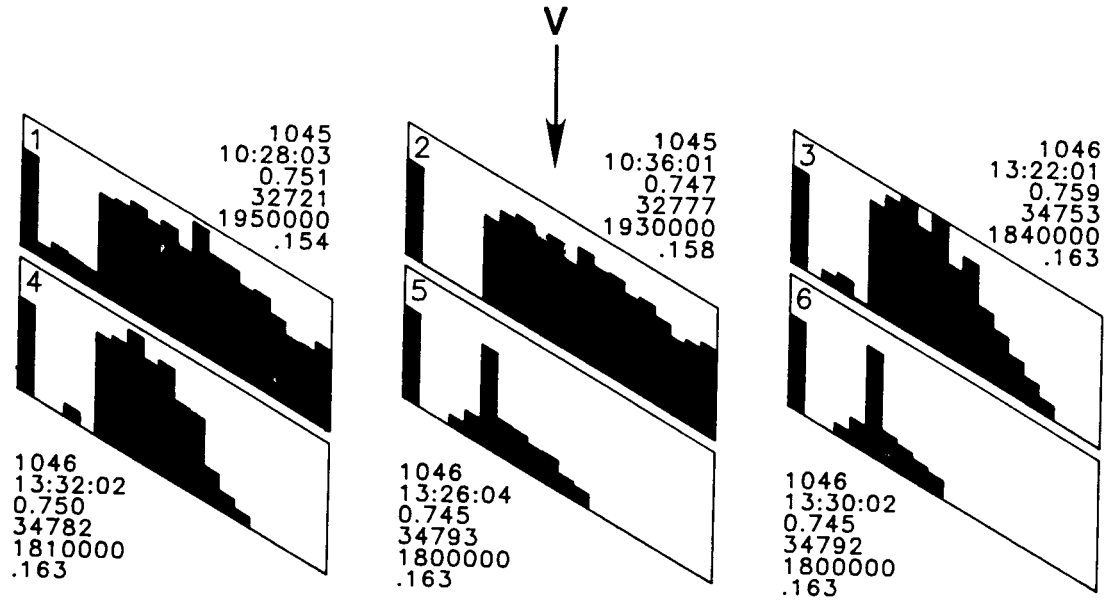

Figure 21. Spanwise turbulence contamination from insect impacts for flights 1045 and 1046.

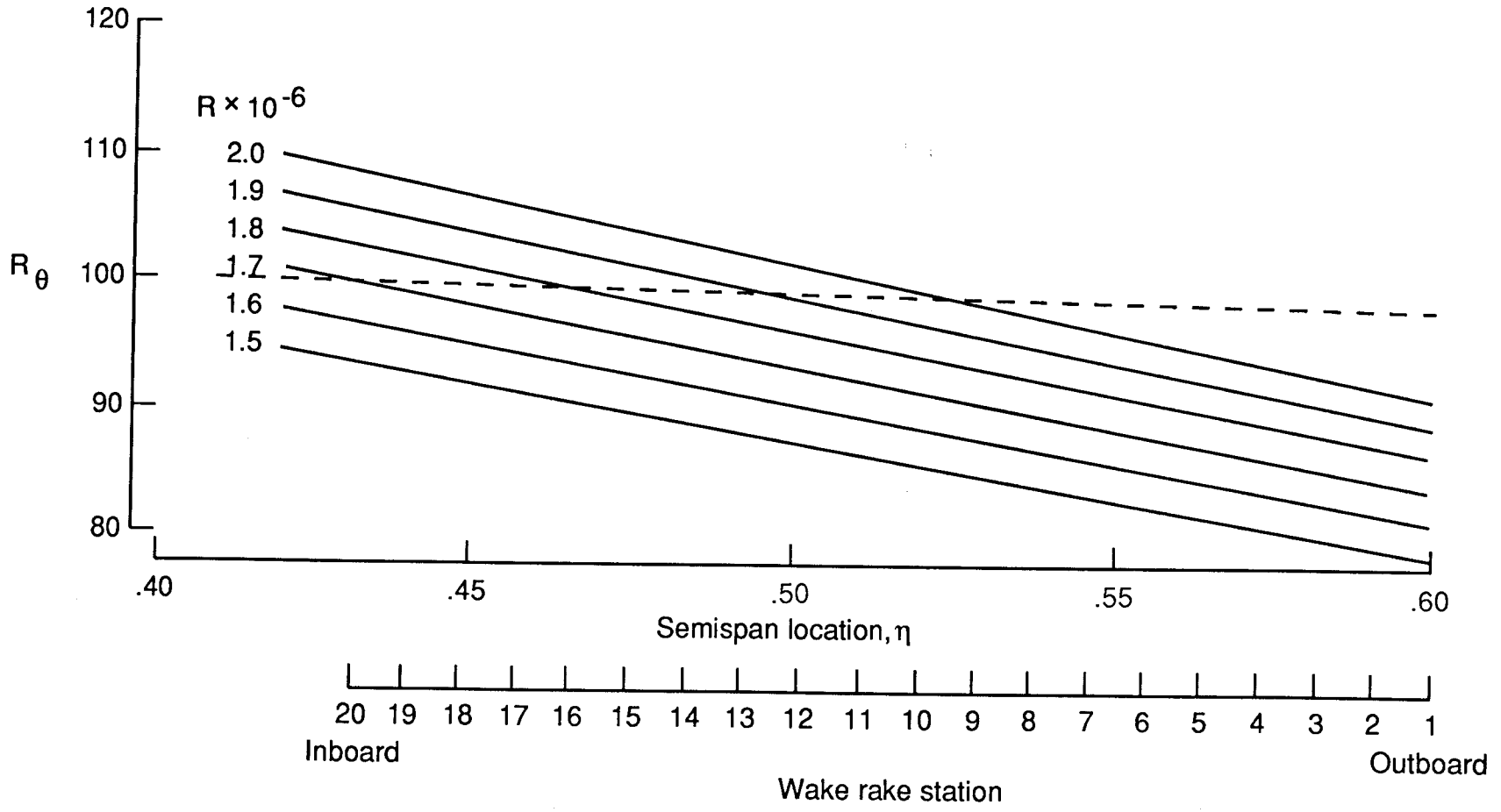

Figure 22. Variation of attachment-line momentum-thickness Reynolds number with spanwise location at design Mach number and suction coefficient.

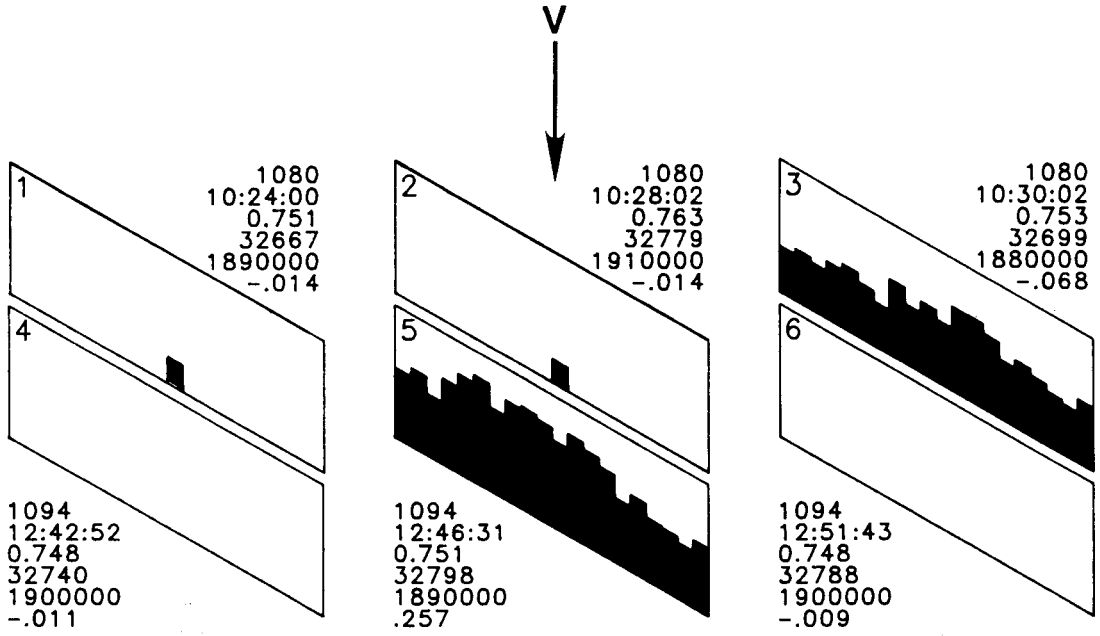

Figure 23. Effects of atmospheric ice crystals for flights 1080 and 1094.

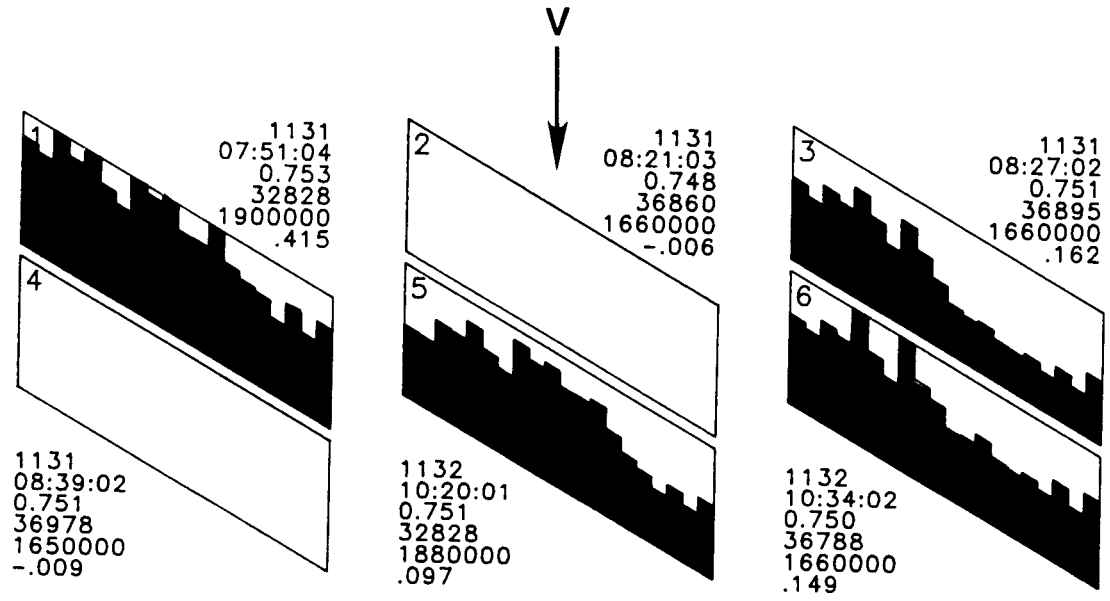

Figure 24. Effects of atmospheric ice crystals for flights 1131 and 1132.

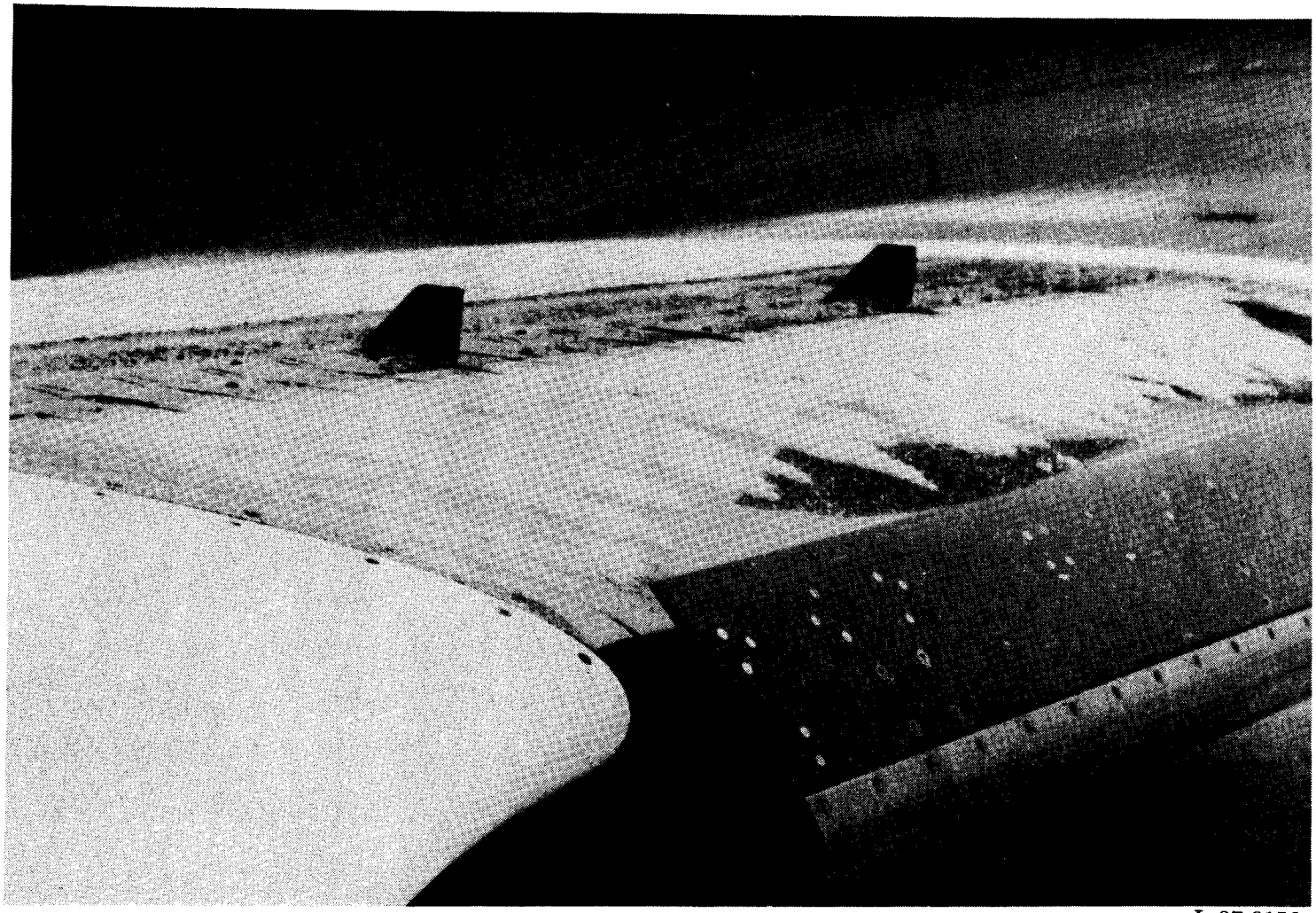

L-87-8156

Figure 25. Overnight accumulation of snow and ice at Cleveland, Ohio.

L-87-8155

Figure 26. Use of hand-held deicer.

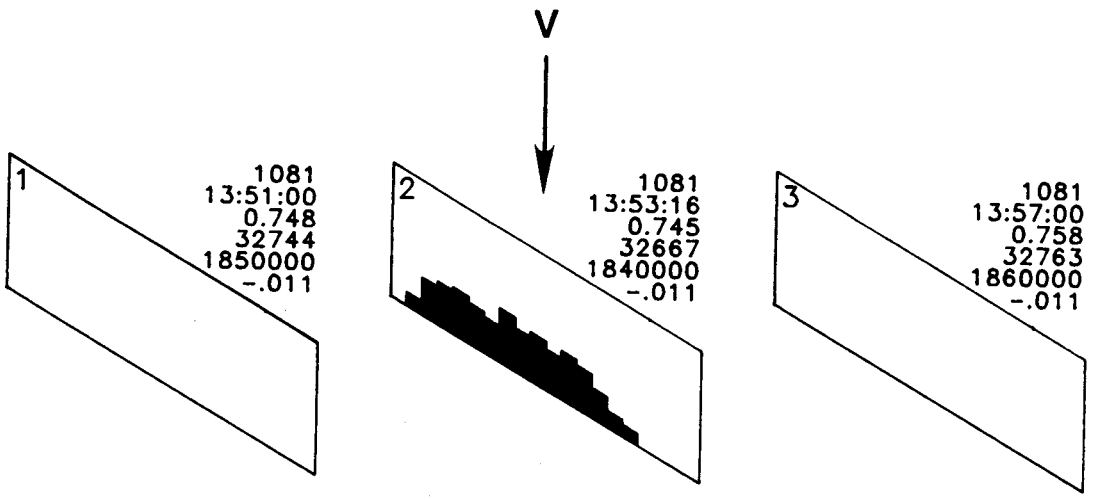

Figure 27. Effect of short-duration angle-of-attack changes for flight 1081; free-stream turbulence of $\pm 0.1g$ for planform 2.

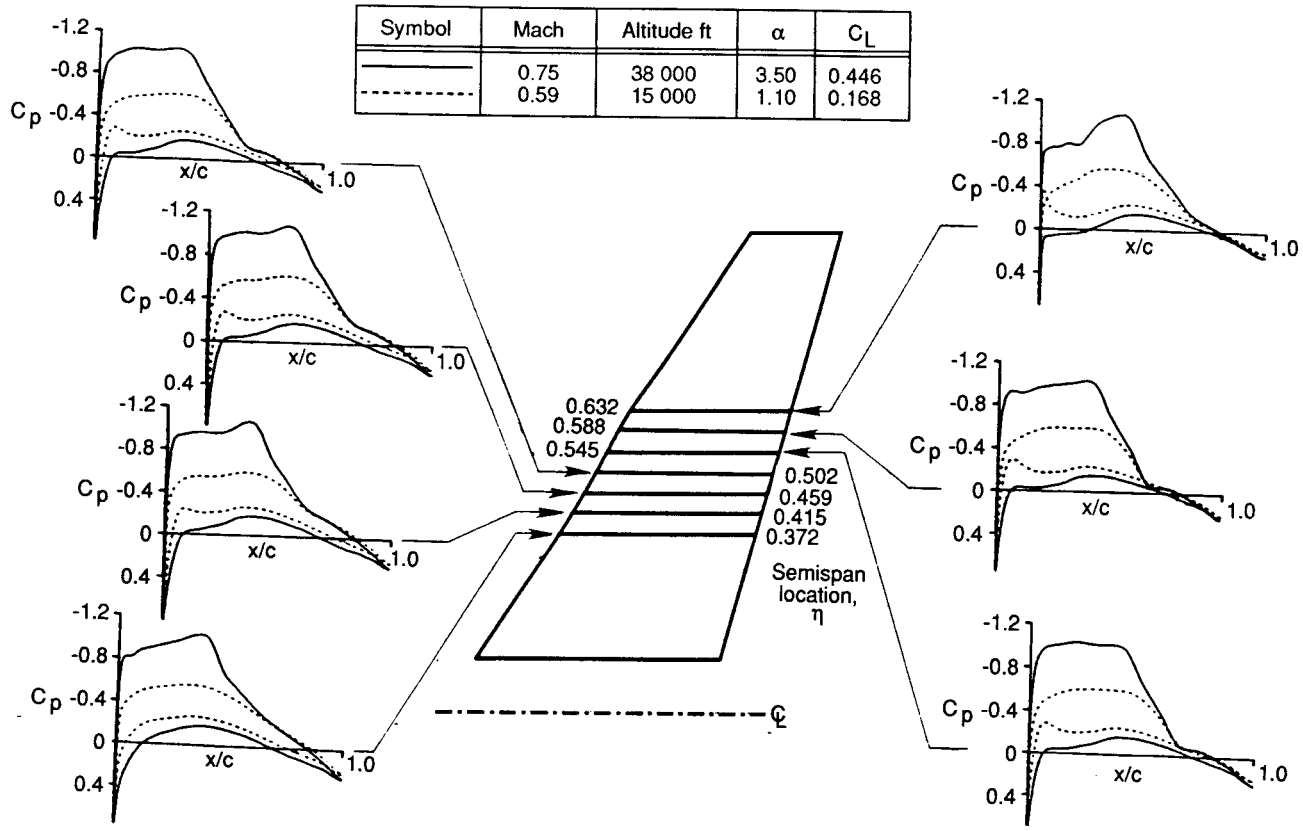

Figure 28. Predicted spanwise pressures on leading-edge test article at cruise and at low-altitude flight.

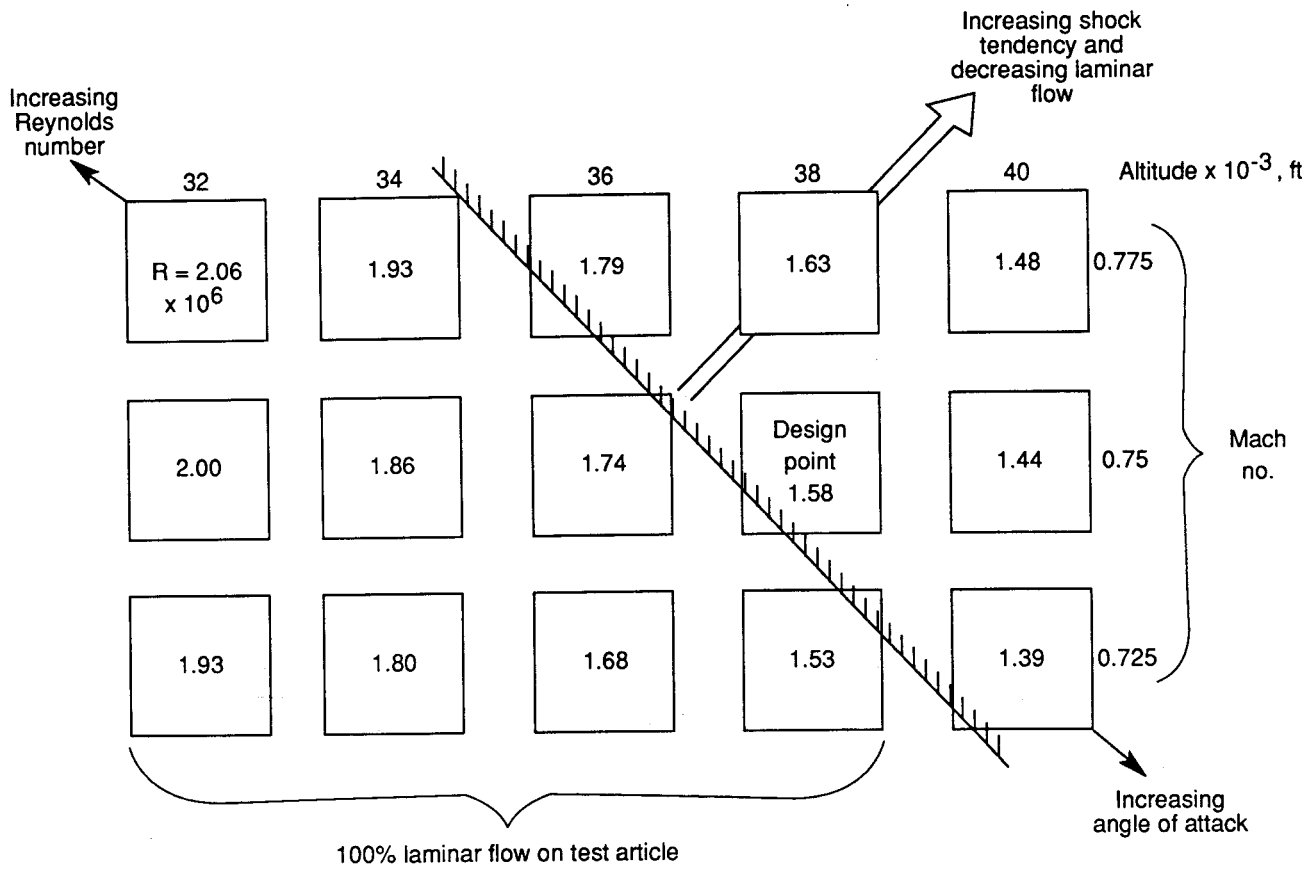

Figure 29. JetStar flight-test conditions.

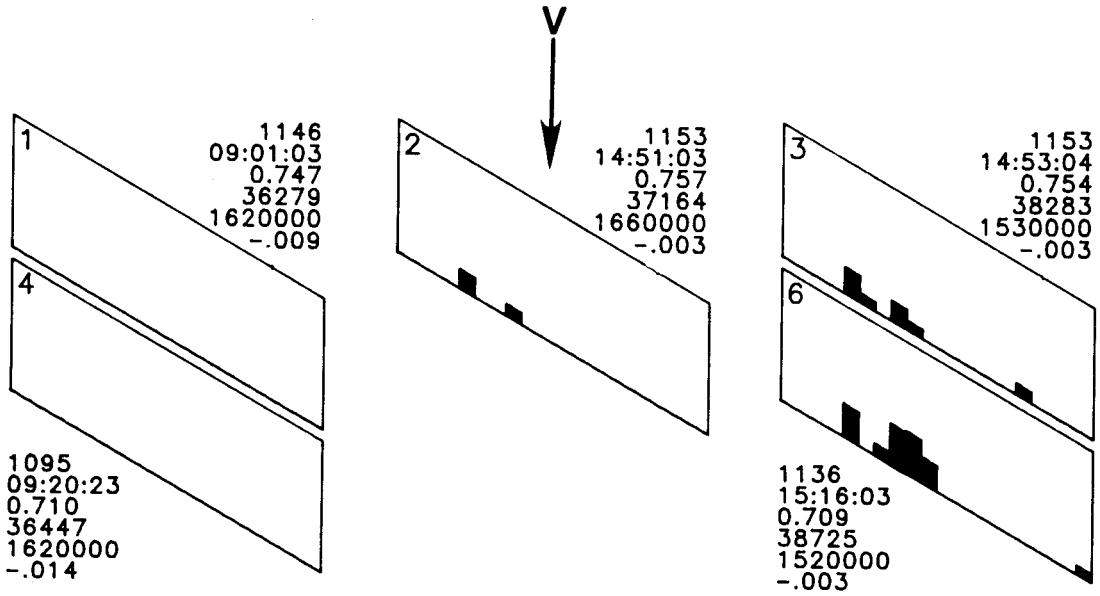

Figure 30. Adverse Mach number effects for flights 1095, 1136, 1146, and 1153.